(2)

NAVAL POSTGRADUATE SCHOOL
Monterey, California

THESIS

COASTAL BOUNDARY LAYER AND REFRACTIVITY MEASUREMENTS USING THE GROUND-BASED HIGH RESOLUTION INTERFEROMETER SOUNDER (GB-HIS)

by

Roy R. Ledesma

December, 1993

Thesis Advisor: Carlyle H. Wash

Approved for public release; distribution is unlimited.

REPORT DOCUMENTATION PAGE

Form Approved OMB No. 0704

1. AGENCY USE ONLY *(Leave blank)*	2. REPORT DATE December 1993	3. REPORT TYPE AND DATES COVERED Master's Thesis

4. TITLE AND SUBTITLE
COASTAL BOUNDARY LAYER AND REFRACTIVITY MEASUREMENTS USING THE GROUND-BASED HIGH RESOLUTION INTERFEROMETER SOUNDER (GB-HIS)

5. FUNDING NUMBERS

6. AUTHOR(S) Roy R. Ledesma

7. PERFORMING ORGANIZATION NAME(S) AND ADDRESS(ES)
Naval Postgraduate School
Monterey CA 93943-5000

8. PERFORMING ORGANIZATION REPORT NUMBER

9. SPONSORING/MONITORING AGENCY NAME(S) AND ADDRESS(ES)

10. SPONSORING/MONITORING AGENCY REPORT NUMBER

11. SUPPLEMENTARY NOTES The views expressed in this thesis are those of the author and do not reflect the official policy or position of the Department of Defense or the U.S. Government.

12a. DISTRIBUTION/AVAILABILITY STATEMENT
Approved for public release; distribution is unlimited.

12b. DISTRIBUTION CODE
*A

13.
ABSTRACT *(maximum 200 words)*

Timesections of potential temperature, dewpoint temperature, modified radar refractivity (M), and the vertical derivative of the modified radar refractivity (dM/dZ) from radiosondes and the Ground-based High Resolution Interferometer (GB-HIS) during three experiments are studied to analyze refractive effects in the coastal boundary layer and evaluate GB-HIS performance. In May of 1991 and 1992, the GB-HIS instrument was deployed on the Research Vessel Point Sur during research cruises off the central California coast. In August and September of 1993, the GB-HIS was deployed during the Variation of Coastal Atmospheric Refractivity (VOCAR) experiment at the Naval Air Station in Point Mugu, California. Comparisons of radiosonde observations with GB-HIS retrievals during the three experiments show that the GB-HIS is capable of depicting large-scale air mass changes in the coastal boundary layer with high temporal resolution. As a result the general location of some refractive layers in the coastal boundary layer can be determined with the GB-HIS data. Small scale features in the moisture timesections from the raob data were not resolved by the GB-HIS with significant skill. The inability of the GB-HIS to capture the vertical moisture gradients seriously limits its ability to monitor refractive conditions.

14. SUBJECT TERMS: Remote Sensing, Coastal Meteorology, Interferometer, Atmospheric Profiling

15. NUMBER OF PAGES 82

16. PRICE CODE

17. SECURITY CLASSIFICATION OF REPORT	18. SECURITY CLASSIFICATION OF THIS PAGE	19. SECURITY CLASSIFICATION OF ABSTRACT	20. LIMITATION OF ABSTRACT
Unclassified	Unclassified	Unclassified	UL

Approved for public release; distribution is unlimited.

Coastal Boundary Layer and Refractivity Measurements
Using the Ground-Based High Resolution Interferometer Sounder (GB-HIS)

by

Roy R. Ledesma
Lieutenant, United States Navy
B.S., United States Naval Academy, 1987

Submitted in partial fulfillment
of the requirements for the degree of

MASTER OF SCIENCE IN METEOROLOGY AND
PHYSICAL OCEANOGRAPHY

from the

NAVAL POSTGRADUATE SCHOOL
December 1993

Author: 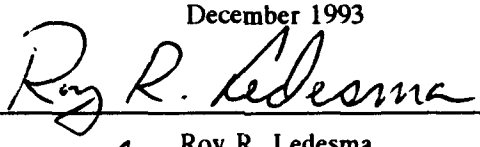

Roy R. Ledesma

Approved by: 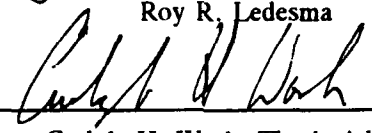

Carlyle H. Wash, Thesis Advisor

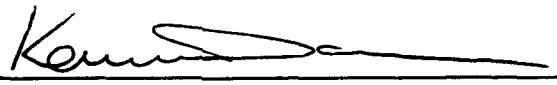

Kenneth L. Davidson, Second Reader

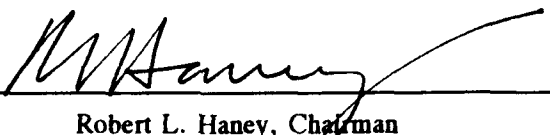

Robert L. Haney, Chairman
Department of Meteorology

ABSTRACT

Timesections of potential temperature, dewpoint temperature, modified radar refractivity (M), and the vertical derivative of the modified radar refractivity (dM/dZ) from radiosondes and the Ground-based High Resolution Interferometer Sounder (GB-HIS) during three experiments are studied to analyze refractive effects in the coastal boundary layer and evaluate GB-HIS performance. In May of 1991 and 1992, the GB-HIS instrument was deployed on the Research Vessel Point Sur during research cruises off the central California coast. In August and September of 1993, the GB-HIS was deployed during the Variation of Coastal Atmospheric Refractivity (VOCAR) experiment at the Naval Air Station in Point Mugu, California. Comparisons of radiosonde observations with the GB-HIS is capable of depicting large-scale air mass changes in the coastal boundary layer with high temporal resolution. As a result, the general location of some refractive layers in the coastal boundary layer can be determined with the GB-HIS data. Small scale features in the moisture timesections from the raob data were not resolved by the GB-HIS with significant skill. The inability of the GB-HIS to capture the vertical moisture gradients seriously limits its ability to monitor refractive conditions.

TABLE OF CONTENTS

ACKNOWLEDGMENTS

I would like to express my deepest thanks to Dr. Carlyle Wash, my thesis advisor, for his enthusiasm and guidance throughout the course of my thesis. I was continually at his door and he was always willing to offer advice along with some much needed encouragement. Thanks also go to Dr. Ken Davidson for sharing his expertise in the area of refraction with me. I am also very grateful to Miss Mary Jordan and Mrs. Tamar Neta without whose programming expertise, I would not have completed this thesis on time. In the IDEA lab, much help was received from Mr. Jim Cowie and thanks goes to him as well. Finally, I dedicate this finished work to my wife, Sharon, and thank her for her love, support and encouragement all those days I was busy working on this thesis.

I. INTRODUCTION

The Navy is changing in response to the challenges of a new global political environment. The shift in strategic landscape, from open ocean to littoral, significantly effects the operation and performance of modern naval weapon systems, sensors and communications. Coastal meteorology is characterized by constantly changing environmental conditions. Atmospheric parameters such as air temperature, water vapor, and aerosols must be measured continuously to assess this changing environment. Also, there is a need to continuously estimate tactical parameters such as refractivity to enhance the performance of weapon systems, sensors and communications.

The Ground-Based High-Resolution Interferometer Sounder (GB-HIS) continuously measures the infrared spectrum (3.3 - 18.2 μm) passively with very high spectral resolution providing near-continuous temperature and water vapor profiles throughout the lower troposphere over land and in a coastal marine environment (Smith et al., 1992). The GB-HIS is capable of measuring marine temperature inversions and surface moisture gradients within the planetary boundary layer and consequently has the potential for determining abrupt changes and boundaries in refractivity conditions. Knowing the location and time of occurrence of marine inversions that

cause electromagnetic ducts aloft enhances the performance of shipboard sensors and communications systems.

During the past several years, GB-HIS data have been successfully gathered in numerous field experiments. The data used in this thesis are from (1) a research vessel, Point Sur (PTSUR), off the coast of central California on 8-10 May 1991 and 9-10 May 1992, and (2) the Naval Air Station at Point Mugu, California during the Variation of Coastal Atmospheric Refractivity (VOCAR) experiment when the GB-HIS was located on the coast from August to September 1993. The data from the three experiments were averaged over ten minute time intervals to reduce both the data volume as well as the radiometric noise. In situ radiosonde data was gathered at approximately 3 to 6 hour intervals to validate the GB-HIS and to better understand the coastal environment.

The objective of this thesis is twofold. The first is to do a military assessment on the GB-HIS retrievals from the PTSUR 1991 and 1992 cruises and the 1993 VOCAR (PTMUGU) experiment by comparing GB-HIS retrievals with radiosonde data and illustrating the strengths and weaknesses. The second objective is to use the combined GB-HIS and radiosonde data to describe the evolution of refractivity in a coastal atmosphere for three different experiment periods.

Chapter II describes the capabilities of the GB-HIS instrument. Chapter III summarizes past GB-HIS performance as compared to other sounding devices and at different times and

locations. Chapter IV provides a refractivity analysis on the GB-HIS data during the three field experiments previously mentioned. Finally, Chapter V presents conclusions and recommendations for further studies.

II. THE GB-HIS INSTRUMENT

A. INSTRUMENT CHARACTERISTICS

1. HARDWARE

The High Resolution Interferometer Sounder (HIS) is a passive infrared remote sensing device that has been deployed on satellites, aircraft as well as on the ground. As a ground-based instrument, the GB-HIS measures downwelling electromagnetic radiation across a near-continuous infrared spectrum to produce relatively high resolution vertical temperature and moisture profiles within the planetary boundary layer (Smith et al., 1992). The current version of the GB-HIS allows for simultaneous monitoring of both longwave (15 μm) and shortwave (4.3 μm) carbon dioxide and water vapor channels. Additionally, the GB-HIS is capable of detecting clouds during partly cloudy conditions as well as determining the amount of marine aerosols (visibility) present in the planetary boundary layer.

The GB-HIS uses interference to produce the detailed spectral data. Although there are numerous methods used for achieving the desired spectral separation of incident radiation (absorption, reflection, dispersion, interference, transmission), interference is the method most commonly used. If two waves are 180 degrees out of phase, the result is

destructive interference. Conversely, if two waves are in phase, there is constructive interference. Interferometers vary the path length between two or more beams by different amounts to obtain alternate intervals of constructive and destructive interference (Rao et al., 1990). Figure 1 illustrates this beam splitting mechanism.

The GB-HIS developed at the University of Wisconsin is a Michelson interferometer which passively measures the downwelling infrared radiance spectrum (3.3-18.2 μm) continuously. The radiance spectra are transformed to atmospheric temperature and water vapor profiles at a spectral resolution of 0.5 cm^{-1} ($\lambda/\delta\lambda>1000$) within the planetary boundary layer (0-2 km). Using an atmospheric radiation model to relate infrared wavelength and atmospheric optical depth, atmospheric state parameters which provide the "best fit" to the measured radiance are derived from the downwelling spectra. The measurement technique combines state of the art radiometric observations and sophisticated nonlinear least squares fitting to obtain the vertical profiles needed to study atmospheric refractivity (Knuteson, 1993).

2. SOFTWARE

The GB-HIS evolved from the aircraft prototype of a new generation satellite sounder (Smith et al., 1990; Revercomb et al., 1988). The prototype, "Baby HIS", is a single detector (5-20 μm) BOMEM-120 interferometer. The

second generation ground-based system, the Atmospheric Emitted Radiance Interferometer (AERI), has a two detector (5-20 μm and 3-5 μm) BOMEM-100 interferometer. The latest and most advanced version of the GB-HIS , AERI-01, is a two detector (5-20 μm and 3-5 μm) BOMEM-100 interferometer with a liquid nitrogen autofill system and a substantially improved version of the retrieval software which allows for: (1) simultaneous use of both longwave (15 μm) and shortwave (4.3 μm) carbon dioxide and water vapor channels, (2) greatly improved cloud detection allowing retrieval during partly cloudy conditions, and (3) retrieval of marine aerosol amount (visibility). Data from all three instruments will be studied in this thesis. The prototype, "Baby HIS", was used during the 1991 PTSUR cruise and the AERI was used during the 1992 PTSUR cruise. AERI-01 was deployed during the 1993 VOCAR (Variation of Coastal Atmospheric Refractivity) experiment.

The GB-HIS measures the downwelling infrared radiance on an automated schedule. The time interval between measured spectra is about ten minutes in which every measured spectrum could potentially provide an atmospheric sounding. Figure 2 visually shows infrared atmospheric transmittance with respect to wavelength and the types of gases that can be measured in these infrared bands. The 15 μm CO_2 absorption band is the primary band for temperature sounding, the combined 4.3 μm CO_2 and 4.5 μm N_2O bands are used to enhance the temperature

resolution in the lower troposphere while the 6.7 μm H_2O absorption band gives moisture measurements.

In clear conditions, the GB-HIS measures radiance spectra for the entire low troposphere. If a cloud layer is present, the GB-HIS determines the temperature and dewpoint profiles from the surface to the cloud base.

3. CALIBRATION

Calibration of the HIS is conducted once per minute using two high emissivity cavity blackbodies, one controlled at 333 K and the other which maintains the ambient temperature (280-295 K), and a third calibration source of a liquid nitrogen bath at 77 K. The scene switching mirror is controlled by a processor to spend a preselected amount of time viewing the atmosphere and any of the calibration positions (Smith et al., 1992).

B. TACTICAL APPLICATIONS

An attractive feature of the GB-HIS is its simplicity and low cost. The GB-HIS can be purchased at less than $30,000. For a complete system, which includes an automated calibration facility and a data processing and dissemination system, the cost would be less than $50,000 (Ding, 1993).

In addition to its low cost, the GB-HIS has great tactical significance. Refractivity measurement is a critical environmental parameter for the assessment of radar performance on small combatants, especially during independent

ship operations. Currently, the operational availability of the refractivity measurement is usually only on large combatants by meteorological operators using balloon launched radiosonde systems. These systems are limited by the required special and heavy equipment (helium tanks), the overt radio transmissions of the sonde, and the technical applicability of how often and in what environmental situations that refractivity measurements need to be taken. On the other hand, the GB-HIS is a multi-channel infrared sensor that operates in a continuous mode, passively, and with small size and weight.

III. GB-HIS PERFORMANCE

A. COMPARISON WITH OTHER SOUNDING DEVICES

There have been several highly successful experiments conducted with the GB-HIS in dry environments to obtain temperature and water vapor profiles. Experiments such as the Ground-based Atmospheric Profiling Experiment (GAPEX), conducted in Denver, Colorado during October and November 1988, and the Spectral Radiation Experiment (SPECTRE), conducted in Coffeyville, Kansas during November and December 1991, demonstrated that the GB-HIS could retrieve temperature and water vapor profiles with significant skill (Smith et al., 1990 and Ding, 1993).

1. GAPEX 1988

The GB-HIS data can be best analyzed by comparisons with other sounding devices. During GAPEX, the GB-HIS was compared to three other state-of-the-art sounding systems. The sensors included a six-channel, passive Microwave Profiler (MWP), an active Radio Acoustic Sounding System (RASS), and a Cross-Chain Loran Atmospheric Sounding System (CLASS). The CLASS was used as the control for the experiment to provide research-quality in situ thermodynamic observations to verify the accuracy and resolution characteristics of each of the three remote sensors (Smith et al., 1990). On 1 November

1988, all four sounding systems were operated simultaneously at 3 h intervals with the MWP and the GB-HIS data recorded continuously throughout the 24 h period. The GB-HIS observations were obtained using the developmental airborne instrument, the "Baby HIS", looking upward. A modified airborne instrument algorithm was used to retrieve the data. This algorithm was not tailored for an upward-looking surface observation.

Even though the developmental airborne HIS was not designed to look upward from the surface, Fig 3 shows extremely good agreement between radiance spectra observed with GB-HIS and radiance spectra calculated using a regression atmospheric transmission model based on Fast Atmospheric Signature Code (FASCODE) (Clough et al., 1988) and a CLASS sounding of temperature and water vapor. There does exist a minor difference between the observed and calculated radiance spectra in the window region between 800 and 1000 cm^{-1} (10-12.5 μm) due to the emission of Freon 11 and 12 which was not included in the FASCODE calculation.

Figure 4 illustrates temperature profiles observed by each sensor within the 850-650 mb layer at 3 hour intervals. All three sounding systems appear able to sense temperature to within 1°C of the CLASS verification data. Differences between the sounding systems arise near 820 mb (top of the surface inversion layer) and near 650 mb. Note that the GB-

HIS/CLASS discrepancies do not increase as rapidly with height as do the discrepancies of the MWP with CLASS. This may be attributed to the larger number of spectral channels possessed by the GB-HIS as compared to the MWP. Figure 5 shows that the closest overall agreement between the CLASS verification and the MWP, GB-HIS and RASS temperature profiles in rms difference is between the CLASS and GB-HIS. Comparison of the three sounding systems' errors with the standard deviation of the CLASS data demonstrates that all three systems possess significant skill at defining lower tropospheric temperature variations (Smith et al., 1990).

Water vapor profile information can also be retrieved from GB-HIS radiance spectra due to the large number of water vapor emission bands. The retrieval of water vapor structure from upward looking passive radiometer measurements is difficult because of the dominating influence of near surface atmospheric emission which, in the case of water vapor, is accentuated by the exponential decay of mixing ratio with altitude (Smith et al., 1990). Figure 6 shows the 3 h tendency of dew-point temperature estimated from GB-HIS spectral radiance as compared to that observed with CLASS. GB-HIS does show significant skill in describing the 3 hour changes below the lowest kilometer.

2. SPECTRE 1991

During SPECTRE, GB-HIS data was successfully collected for 11 days. Most of the days were cloudy but there were some clear days. The RMS errors for temperature from this experiment were within 1.0 K between 700 - 990 mb increasing to 1.5 K at the surface. RMS errors for dewpoint temperatures were less successful. Departures from the radiosondes were greater than 5.0 K at the surface and near 3.0 K from 980 mb to 700 mb (Ding, 1993).

B. COMPARISON AT DIFFERENT TIMES AND LOCATIONS

1. PTSUR 1991

Recently, GB-HIS measurements can be made in the coastal zone to test the viability of this instrument in the presence of high, low-level moisture. In May 1991, a research cruise was conducted by the Naval Postgraduate School onboard the Research Vessel (RV) Point Sur. The purpose of this cruise was to validate the performance of the GB-HIS in a coastal marine environment.

a. RADIANCE ANALYSIS

Revercomb et al., (1993) compared GB-HIS 1991 observations from Denver, CO and Monterey, CA. On 28 February 1991 in Denver, Colorado, the "Baby HIS" was used with a retrieval algorithm which accounted for the influence of clouds. This algorithm enabled boundary layer profile determinations under all cloud conditions. Figure 7 shows the

radiance spectra obtained by the GB-HIS on 28 February 1991 at 1217Z in Denver, Colorado. The three regions of the radiance spectrum are:

1. 500 - 600 cm^{-1} (20 - 16.8 μm): **rotational water vapor band** - useful in upper air moisture retrieval for a dry atmosphere and in lower air moisture retrieval for a coastal/marine atmosphere

2. 600 - 770 cm^{-1} (16.8 - 13 μm): **15 μm CO_2 band** - useful in temperature retrieval

3. 770 - 1400 cm^{-1} (13 - 7 μm): **water vapor continuum** -useful in water vapor retrieval

The spectral resolution is 0.5 cm^{-1}. The "M" shaped feature centered near 1040 cm^{-1} (9.6 μm) is the IR ozone emission. The concave shape of the 15 μm CO_2 band (600 - 700 cm^{-1}) indicates a strong low level temperature inversion. This concave shape is present in the radiance spectra because the spectral shape of the CO_2 band corresponds to the vertical shape of the temperature variance within the 1000-800 mb layer. Smith et al., (1992) states that the radiance tends to first increase with somewhat weaker absorption away from the CO_2 band center (667 cm^{-1} or 15 μm) and then decreases abruptly corresponding to the decrease in temperature above the inversion layer (620 cm^{-1} or 16.1 μm). Compare Fig 7 with Fig 8 illustrating another radiance spectra obtained at 0607Z on 28 February 1991 in Denver, Colorado. At this time, there is no low level inversion present as indicated by the convex shape of the CO_2 band. The radiance tends to decrease away from the opaque

center of the CO_2 band in a low tropospheric temperature lapse situation.

Similar results were obtained in Monterey, California on 7 May 1991. At 1445 local time, the GB-HIS, operating on the research vessel, Point Sur, obtained the radiance spectra shown in Fig 9. The slight concave shape of the CO_2 band indicates the presence of a low level inversion. This inversion indicated by the GB-HIS corresponds with radiosonde observation (Fig. 10). Conversely, Fig 11 shows the radiance spectra observed at 1700 local time on 9 May 1991 when no low level inversion existed. This spectrum was taken off the coast south of Monterey after a frontal passage on the previous day. Note the convex shape of the CO_2 band which indicates no inversion is present.

In comparison to the radiance spectra taken in Denver during a period of a low level inversion, the radiance spectra observed in Monterey on 7 May 1991 shows that the water vapor continuum lines and the rotational water vapor lines are much stronger than in the Denver case. More information exists in the Monterey spectrum. Conversely, the low level of the water vapor continuum and the smaller water vapor lines on 9 May 1991 in Monterey indicate a drier atmosphere. Figure 12 is the radiosonde observation from 9 May 1991 and it corresponds quite well with radiance spectra observed by the GB-HIS.

At 1100 local time on 9 May 1991 in Monterey, a low cloud deck was observed by the GB-HIS as shown in Fig 13. The presence of low level clouds produces a higher radiance value from the cloud emission across the complete spectrum. Notice that information is still available in the CO_2 and water vapor bands by the amplitude of spikes in the spectrum.

b. RETRIEVAL ANALYSIS

Rugg (1992) found the following strengths of the GB-HIS during the 1991 Point Sur cruise: (1) the ambient temperature was within 3 °C of rawinsonde data, (2) there was good agreement in the vertical temperature and moisture structure throughout the low troposphere on the 9th of May. The GB-HIS also displayed the general observed trend of boundary layer cooling as the cold front approached and passed. The most notable weakness was that specific narrow moisture layers were not captured and a number of the details in the thermal structure were not well described. Specifically, on 8 May 1991, the pronounced drying was analyzed to be too dry and too early and the behavior of the marine inversion and its collapse as the front approached is depicted differently by the GB-HIS retrievals. The rms dewpoint differences are quite small near the surface (below 970 mb) with values below 1.5 K but above 970 mb, the rms dewpoint differences increase dramatically to 21.0 K (Rugg, 1992). More examples of these boundary layer features,

particularly as they apply to atmospheric refractivity, will be discussed in the next chapter.

2. PTSUR 1992

a. *RADIANCE ANALYSIS*

In May 1992, a research cruise was completed by the Naval Postgraduate School to continue the validation of the GB-HIS in a marine environment. The GB-HIS instrument used on the 1992 cruise was the second generation (AERI) two channel interferometer. The spectral resolution continued to be 0.5 cm^{-1}. The radiance spectra observed during the Point Sur cruise show the strong effect of the frequent coastal marine inversion. Figure 14a illustrates the radiance spectra obtained at 0257Z on 10 May 1992. The concave shape of the CO_2 band indicates that a strong low level inversion is present. Figure 14b (which is a blow-up of Fig. 14a) suggests that an elevated inversion exists (14.0-13.4 μm). The low level of the water vapor continuum and the larger amplitude in the rotational water vapor absorption lines (20-18 μm) indicates a drier atmosphere as compared to the radiance spectra of 0000Z on 10 May 1992 (Fig. 15). Smith et al., (1992) states that for a given atmospheric temperature structure, the smaller the concentration of water vapor, the greater the amplitude of the rotational water vapor absorption lines. The shape and level of the water vapor continuum (13-7 μm) shows that the atmosphere is not transparent and there

exists absorption and emission of aerosols and water vapor which prevents the water vapor continuum to reach zero. The absence of strong water vapor continuum absorption lines suggests a drier atmosphere. Also, if the water vapor continuum level is low, then no clouds will be present.

However, if the radiance spectra resembles the Plank curve, then a very moist and overcast atmosphere is expected. This is illustrated by, Fig 16, the radiance spectra from 1700Z on 10 May 1992. Note the resemblance of the spectra to the Plank curve. There are no strong water vapor absorption lines nor a distinguishable CO_2 absorption band. This radiance spectra indicates an overcast of low marine stratus clouds which agrees with the observed weather for this time.

b. RETRIEVAL ANALYSIS

Rugg (1992) found that the most obvious strength of the GB-HIS retrievals in comparison with the rawinsonde soundings was the detection of the marine temperature inversion throughout the entire 1992 cruise. The GB-HIS detected fluctuations in the inversion height and strength such as the inversion layer change on 10 May 1992 from 1400Z to 1900Z which was related to the stratus overcast shown in the radiance spectra (Fig. 16). The GB-HIS depicted the relative strength of the marine inversion to within 2-3 K of

the rawinsonde for the inversion top. The surface moist layer was also well depicted by the GB-HIS.

The most notable weakness of the GB-HIS retrievals during the 1992 cruise was again the depiction of small scale features in the moisture profiles. Specifically, on 9 May 1992 between 00Z and 03Z where sharp moist and dry layers were depicted within 100 mb by the rawinsonde and not the GB-HIS. Other weaknesses were 1) a weaker moisture gradient from the surface to the base of the inversion, 2) a continuous and weaker temperature gradient from the surface to the top of the inversion, 3) a tendency to overestimate the height of the top of the inversion, and 4) an overestimation of the moisture near the surface. Smith et al., (1990) also found relatively large errors in this portion of the atmosphere (700-1000 mb). From the 1991 and 1992 Point Sur cruises, Rugg (1992) and Ding (1993) concluded from an error analysis of GB-HIS soundings that an accuracy of 1.0 degree K for temperature and 3.0 degree K for dew point, respectively, can be achieved in clear conditions with the GB-HIS sounding system. Additionally, it is evident that the observed radiance spectrum by the GB-HIS in the rotational water vapor absorption band (20-16.7 μm), the CO_2 absorption band (16.7-13.0 μm), and the water vapor absorption continuum (13.0-6.9 μm) contain detailed information on the atmospheric temperature and moisture and

this information can be retrieved in the lower tropospheric layer in clear conditions.

3. PT MUGU 1993 (VOCAR)

During the VOCAR (Variation of Coastal Atmospheric Refractivity) experiment conducted in August 1993 at the Naval Air Station in Pt Mugu, California, the GB-HIS operated alongside a Microwave Profiler system (MWP), a SODAR system and a LIDAR system, which are active remote sensing devices. The MWP transmits microwave energy, SODAR transmits sound energy, and LIDAR transmits light energy to observe the structure of the planetary boundary layer.

a. RADIANCE ANALYSIS

A three day period (26-28 August 1993) during the VOCAR experiment was identified as being a good period for analysis of GB-HIS data. The radiance spectra for these days showed nearly cloud-free atmosphere with a persistent elevated inversion and strong marine layer. Figure 17 presents the radiance spectrum for 0400Z on 26 August 1993. The strong rotational water vapor absorption lines between 20 μm and 16.7 μm and the stronger absorption lines in the water vapor continuum (13.0-6.9 μm) define the strong marine moisture layer. The low level of the water vapor continuum suggests a nearly cloud-free condition. Also, the concave shape of the CO_2 band suggests the presence of a low level inversion in addition to the elevated inversion which is depicted by the

pronounced spikes between 14 μm and 13.4 μm as illustrated in Fig 18.

b. RETRIEVAL ANALYSIS

Radiosondes were launched at Pt Mugu every 4 hours daily beginning at 00Z during this period. The GB-HIS observations were at approximately 10 minute intervals and therefore have a 24 times higher temporal resolution than the raob. However, the GB-HIS measurements are derived from the passive infrared and have an inherently less vertical resolution as compared to the in-situ raob. The retrieval algorithm used a first guess made from smoothing the 00Z raob for each day to initialize the retrieval at the beginning of each UTC day. Of particular interest are the comparison of the vertical derivative of the modified radar refractivity (dM/dZ) between the radiosonde and the GB-HIS instrument.

IV. REFRACTIVITY ANALYSIS

Examined in this chapter is the ability of the GB-HIS to monitor coastal boundary layer changes and related refractive effects. Specifically, data obtained from three experiments (PTSUR 1991, PTSUR 1992, and PTMUGU 1993) are analyzed. Changes in the boundary layer structure during the PTSUR cruises in 1991 and 1992 and PTMUGU 1993 are due to the passage of coastal and synoptic weather systems and also to the movement of the ship. Since the main objective is to compare the GB-HIS retrievals with the radiosonde observations, the reasons for the boundary layer changes will be discussed but not emphasized. A timesection format will illustrate similarities and differences between the two types of measurements.

Initial guess profiles were created using the 0000Z radiosonde for each day, interpolated to 40 levels (surface to 500 mb). The interpolated version of the 0000Z radiosonde is then smoothed ten times to remove small scale structures that may cause instabilities in the retrievals. The output from this smoothing process is the initial first guess of the retrieval algorithm (Ding, 1993).

A. PTSUR 1991

The R/V Point Sur traversed a track perpendicular to the coast of central California south and west of Monterey, California during the PTSUR 1991 cruise (Fig. 19a). The 1991 cruise began at 07/1800Z and ended at 10/1400Z, providing useful data for investigation between 08/0000Z and 10/1300Z (Rugg, 1992). A complete discussion of the synoptic conditions during the PTSUR 1991 cruise has been provided by Martinez (1991). The GB-HIS instrument that was used on the 1991 cruise was the "Baby HIS", single-channel interferometer which did not have the capability to record surface temperature with the received radiance signal.

1. Observed Features

a. Prefrontal Conditions (08/0000Z-08/1400Z)

During the beginning of the 1991 cruise, a strong, low-level marine inversion is present between 08/0000Z and 08/0600Z. The potential temperature timesection (Fig. 20), constructed from the radiosonde data, illustrates the inversion as a strong stable layer extending from near the surface to above 910 mb. As a surface cold front approaches from the west, the inversion starts to rise (Fig. 20). Surface data indicated a 08/1400Z frontal passage at the ship. Pronounced dry layers above 940 mb at 08/0000Z and at 850 mb on 08/0600Z (Fig. 21) are evident in the dewpoint temperature timesection.

To depict more clearly the presence of trapping conditions in the atmosphere, the modified radar refractive index (M) is used. This modified index is defined as

$$M=77.6\frac{P}{T}-5.6\frac{e}{T}+3.73x10^{5}\frac{e}{T^{2}}+.157z$$

where P = atmospheric pressure (mb)

e = partial pressure of water vapor (mb)

T = atmospheric temperature (K)

z = height (m)

From the above equation, it can be seen that M is dependent on pressure, temperature, and moisture, all of which are measured by the GB-HIS. Due to large coefficients, the moisture dependence is significant.

For a standard atmosphere, M increases with height. Trapping layers are located in regions where M decreases or is constant with height. The location of the top and bottom of a trapping layer is quickly recognized when plotting M as a function of height. The vertical derivative of M (dM/dZ) clearly illustrates the location of trapping layers. Trapping layers form in regions where dM/dZ is negative (dM/dZ < 0).

The modified radar refractive index, M (Fig. 22), and its vertical derivative, dM/dZ (Fig. 23), show a trapping layer at 940 mb on 08/0000Z and a super-refractive layer at 890 mb on 08/0600Z associated with the thermal and moisture vertical structure. These dry layers are very transient features appearing only at one observation time.

b. Postfrontal Conditions (08/1400Z-09/1200Z)

The inversion continues to rise after the frontal passage reaching a maximum height at 800 mb at 09/1200Z. Beneath the inversion, a deep, well-mixed boundary layer develops (Fig. 20). During this period, moisture levels begin to decrease with time as result of the subsiding dry air following the surface cold front. Figure 21 shows the subsiding dry air capping the moist surface air. The drying is particularly intense between 08/1800Z and 08/2100Z. Following the postfrontal subsidence, moisture levels increase until 09/1200Z (Fig. 21).

The distinct change from the stable air ahead of the front to less stable air after the front is the most dramatic change in the temperature timesection (Rugg, 1992). The lifting of the inversion and development of the well-mixed boundary layer eliminated the trapping layers that were present (Figs 22 and 23).

c. Redevelopment of Boundary Layer Inversion (09/1200Z-10/1200Z)

By 10/0000Z, the low marine inversion, present at the beginning of the cruise, redevelops (Fig. 20). During this period, the reestablishment of the marine boundary layer is related to the subsidence associated with the movement of the subtropical high and upper level ridge into the region. As a result, the inversion and the negative vertical dewpoint

temperature gradient cap the marine boundary layer between 09/1800Z and 10/1200Z (Figs. 20 and 21). A super-refractive layer is found at 970 mb on 10/1200Z related to the newly formed inversion (Figs. 22 and 23).

2. GB-HIS Measurements

a. Prefrontal Conditions (08/0000Z-08/1400Z)

The GB-HIS potential temperature timesection (Fig. 24), constructed from GB-HIS soundings at the same times as the radiosondes, successfully analyzes the strong, low-level marine inversion between 08/0000Z and 08/0600Z. At approximately 08/1200Z, the inversion starts to rise as the surface cold front approaches from the west, in good agreement with the raob data. However, the GB-HIS dewpoint temperature timesection (Fig. 25) does not depict the narrow dry layer at 850 mb on 08/0600Z. It does show a moist pocket, dewpoint temperature of 12 °C, from the surface to 960 mb between 08/0300Z and 08/1200Z. This moist pocket is not verified by the sounding data but illustrates the difficulty the GB-HIS has in depicting small scale moisture features.

The GB-HIS timesection of the modified radar refractivity (M) (Fig 26) and its vertical derivative (dM/dZ) (Fig. 26a) indicates a continuous refractive trapping layer is present at 940 mb from 08/0000Z to 08/2100Z as opposed to the more localized features illustrated by the raob data. Although the GB-HIS indicates a trapping region, its vertical

location is in error due to the poor low-level moisture retrieval discussed above.

b. Postfrontal Conditions (08/1400Z-09/1200Z)

The most noticeable feature on the GB-HIS potential temperature timesection (Fig. 24) during this period is the continuous rise of the evenly-spaced theta surfaces. The inversion top is determined to be 820 mb on 09/1200Z in the GB-HIS data as opposed to 800 mb as depicted in the raob data. The development of a deep, well-mixed boundary layer is also depicted by the GB-HIS in good agreement with the observed radiosondes.

During this period, the GB-HIS dewpoint vertical structures differ considerably from that by the radiosonde. The GB-HIS dewpoint temperature timesection (Fig. 25) does show the postfrontal subsidence but its intensity is considerably weaker than observed. The subsidence extends to 950 mb on 08/1800Z. A pronounced dry pocket, which is not measured in the raob data, is depicted by the GB-HIS at 800 mb between 09/0500Z and 09/2200Z. Another error in the GB-HIS dewpoint retrieval is depicting a layer of moist air, dewpoints to 10 °C, near the surface. The observed moisture data shows drier surface conditions with dewpoint temperatures of approximately 4 °C.

The GB-HIS (Figs 26 and 26a) does show trapping occurring very near the surface at 990 mb between 09/0600Z and

10/0000Z as a result of a rapid decrease in moisture above the moist surface layer between 09/0600Z and 09/2100Z from 1000-970 mb. The raob data (Fig. 21 and 23) does not show this rapid decrease in moisture or trapping in this layer.

c. Redevelopment of Boundary Layer Inversion (09/1200Z-10/1200Z)

The most noticeable features evident in the last period in the GB-HIS potential temperature timesection (Fig. 24) are the subsidence inversion with the resulting reestablishment of a shallow marine boundary layer. The GB-HIS retrieval captures these general trends, however the inversion strength is too weak. The GB-HIS resolves the decrease in dewpoints during this period, however a comparison of radiosonde (Fig. 21) and GB-HIS (Fig.25) dewpoints shows considerable differences in the vertical moisture profiles. The GB-HIS, Fig 25, also indicates a pronounced dry layer at 790 mb between 09/1800Z and 09/2100Z that was not present in the raob data. The GB-HIS depiction of an overly-moist surface layer continues during this period.

Thus, the GB-HIS M and dM/dZ timesections (Figs 26 and 26a) continue to show a refractive trapping layer between 09/0600Z and 09/2200Z at 980 mb which is not depicted in the raob data. Also, the GB-HIS does not resolve the observed trapping layer at 980 mb on 10/1200Z.

d. Hourly GB-HIS Retrievals

Hourly GB-HIS retrievals were also computed for timesection analysis to determine if the high frequency GB-HIS data resolves additional boundary layer structure not present in the previous displays. Figure 27 presents the hourly timesection of potential temperature for the PTSUR 1991 cruise. The hourly data is in general agreement with the lower frequency (every 6 h) data. However, the hourly timesections illustrate considerable noise from hour to hour. The amplitude of noise masks any additional mesoscale features in the hourly data. Fig 27 is representative of other hourly timesections; consequently, hourly retrievals are not discussed further.

3. Summary

The analysis of the PTSUR 1991 data shows that the GB-HIS is an effective tool in measuring the marine temperature inversion. It also shows significant skill in describing the evolution of the well-mixed boundary layer after the passage of the surface cold front. However, the GB-HIS does not capture small scale moisture features. In addition, the GB-HIS moisture retrievals in the surface layer are too moist, leading to the analysis of erroneous low-level vertical moisture gradients and refractive layers. Consequently, the GB-HIS did not show significant skill in depicting the trapping layers during the PTSUR 1991 cruise.

B. PTSUR 1992

In May 1992, another research cruise to validate the GB-HIS in a coastal marine environment was completed using the RV Point Sur. The ship track for the 1992 cruise covered an area off the central California coast north and west of Monterey (Fig. 19b). The cruise began at 08/2000Z and ended at 11/1300Z, providing useful data for the 48 h period between 09/0000Z and 11/0000Z. The GB-HIS instrument utilized on the 1992 cruise was the AERI two-channel interferometer. A complete discussion on the synoptic situation during the PTSUR 1992 cruise has been provided by Rugg (1992).

1. Observed Features

a. Northerly winds with clear/scattered skies (09/0000Z-10/1200Z)

At the beginning of the May 1992 cruise, a strong, low-level marine inversion was present between 09/0000Z and 10/1200Z. The potential temperature timesection (Fig. 28) illustrates the regularly-spaced theta surfaces as a strong stable layer extending from 975-945 mb at 09/0000Z to 990-965 mb at 10/1200Z. The dewpoint temperature timesection (Fig. 29) depicts a moist surface layer and the presence of a moist pocket at 900 mb between 09/0800Z and 09/0900Z and strong drying above 980 mb between 09/1600Z and 10/0300Z. As a result of the inversion and the strong drying that occurred during this period, the M and dM/dZ timesections (Figs 30 and

31) illustrate the development of a continuous trapping layer between 975 mb and 960 mb from 09/1000Z and 10/0300Z. Later in the period, the inversion and the refractive layer shift upward to 960-950 mb from 10/0300Z to 10/1200Z.

b. Southerly winds with stratus overcast (10/1200Z-10/1700Z)

The potential temperature timesection, Figure 28, shows that the low-level marine inversion begins to rise in response to a coastal land breeze which the ship encountered the early morning of 10 May 1992. Wind speeds dropped dramatically and changed direction, coming from the southeast. As a result of the land breeze, a stratus overcast slowly moved in and overtook the ship by 10/1700Z. The ship was maneuvered west to escape from under the stratus overcast. By 10/2000Z, the ship returned to scattered skies and the large-scale prevailing northerly wind regime(Rugg, 1992).

Following the lifting of the inversion, the moist surface layer also deepened as depicted in Fig 29. Figures 30 and 31 show that the associated trapping layer also lifts to 925 mb by 10/1600Z.

c. Northerly winds and scattered skies return (10/1700Z-10/2000Z)

After maneuvering the ship from under the stratus overcast, the R/V Point Sur returned to the clear, northerly winds in this short period. Fig 28 shows that the inversion

began to gradually lower with the movement into this air mass. The dewpoint gradient (Fig. 29) drops also follows the lowering of the inversion. The trapping layer (Figs 30 and 31) also lowers to 950 mb by the end of the period. The R/V Point Sur then turned eastward and returned to port. No further data is presented since most of this period was cloudy.

2. GB-HIS Measurements

a. Northerly winds with clear/scattered skies (09/0200Z-10/1200Z)

The GB-HIS potential temperature timesection (Fig. 32) indicates the presence of a low-level marine inversion, weaker than observed. The presence of the inversion is in agreement with the raob data but the position of the inversion at 990-920 mb at 09/0600Z is somewhat higher than the raob data. The periodic oscillation in the raob inversion height is not as pronounced in the GB-HIS timesection.

The GB-HIS dewpoint retrieval (Fig. 33) presents a smoothed depiction of the moisture analysis (Fig. 29). Specifically, the GB-HIS dewpoint temperature timesection (Fig. 33) does not capture the moist pocket at 900 mb between 09/0800Z and 09/0900Z nor any pronounced drying above 980 mb between 09/1600Z and 10/0300Z. In addition, the surface layer is also analyzed to be too moist by the GB-HIS, as in PTSUR 1991.

The GB-HIS shows a trapping layer at 980 mb between 09/2300Z and 10/1300Z (Figs 34 and 35) but does not fully depict the trapping layer that was illustrated in the raob data. The raob data (Figs 30 and 31) illustrates a trapping layers between 980-970 mb earlier, from 09/1000Z to 10/0400Z, and 965-955 mb from 10/0500Z to 10/1300Z.

b. Southerly winds with stratus overcast (10/1200Z-10/1700Z)

With the onset of southerly winds and the stratus overcast, the GB-HIS potential temperature timesection (Fig. 32) indicates a lifting in the marine inversion from 10/0900Z to 10/1700Z. With the rise of the inversion, the moist surface layer, as depicted in Fig 33, also rises slightly. Figure 33 shows strong drying in the GB-HIS results above 940 mb between 10/1400Z and 10/1800Z which is not shown by the radiosondes. This erroneous moisture feature is likely due to clouds affecting the retrieval. The GB-HIS M and dM/dZ timesections (Figs 34 and 35) agree well with the raob data in showing the rise of the trapping layer at 960 mb on 10/1700Z. The GB-HIS depiction of the trapping layer remains lower than that presented by the raob data.

c. Northerly winds with scattered skies return (10/1700Z-10/2000Z)

The GB-HIS theta results, Fig 32, do not show the marine inversion sinking back to its original position with

the return of northerly winds and scattered skies as with the raob data between 10/1700Z and 10/2000Z. However, the GB-HIS dewpoint temperature timesection (Fig. 33) does indicate a moist surface layer sinking back to its original position in agreement with the raob data. The trapping layer is still present at 965 mb at 09/1800Z as depicted in Figs 34 and 35 as compared to 945 mb in the raob data.

3. Summary

The analysis of the PTSUR 1992 data again shows that the GB-HIS can measure the marine temperature inversion with significant skill, although inversion strength is weaker than observed. However, the GB-HIS is not successful in depicting the vertical moisture structure nor the small scale dry and moist layers. As a result, the representativeness of GB-HIS refractivity (M and dM/dZ) timesections were adversely affected. However, the refractivity conditions on 10 May are reasonably described by the GB-HIS. Further, the behavior of the observed trapping layer on 9 May is not captured in the GB-HIS dataset.

C. PTMUGU 1993

In August and September 1993, the University of Wisconsin participated in the Variation of Coastal Atmospheric Refractivity (VOCAR) experiment under sponsorship of the NRL. The VOCAR 1993 experiment was the first field deployment of the AERI-01 system and provided useful data for the study of

the elevated inversion which is such a persistent feature along the California coast. The University of Wisconsin deployed the latest version of the GB-HIS (AERI-01) at the Naval Air Station in Point Mugu, California. The GB-HIS was deployed the week before an intensive observing period (23 August-3 September 1993) and began operation on 18 August 1993 adjacent to the Geophysics building on the Naval Air Station at Point Mugu, California.

A three day period during the VOCAR experiment has been identified as a good period for the initial analysis of GB-HIS data. The 26-28 August 1993 (Z) period was nearly cloud-free with a persistent elevated inversion and strong marine layer. Trapping conditions were indicated from both GB-HIS and radiosonde data. Data from other periods will be available at a later date.

1. Observed Features

a. 26 August 1993

The potential temperature timesection (Fig. 36) indicates the presence of a low-level inversion as a stable layer from 980 mb to 960 mb which weakens during the afternoon. A night-cooling caused a cold pocket of air which is also analyzed at the surface between 26/0600Z and 26/1300Z. Above 960 mb, a diurnal temperature change is present with colder air in the early morning and warmer air in the late afternoon and evening.

The dewpoint temperature timesection (Fig. 37) depicts the capping of the moist surface layer by dry air aloft. A very dry layer is analyzed at 960 mb on 26/0400Z. Above the dry air at 930 mb between 26/1400Z and 26/1800Z, a moist pocket is also analyzed. In the regions where the inversion and rapid drying with height are co-located, a continuous trapping layer develops. Figures 38 and 39 show that the refractive layer is present between 980 mb and 965 mb and lowers as the inversion drops during the day.

b. 27 August 1993

On the 27th, the observed variation in the vertical structure of potential temperature closely resembles the previous day. Figure 36 shows a lifting and strengthening of the inversion between 27/0000Z and 27/1800Z and with a lowering of the inversion between 27/1800Z and 27/2300Z. The diurnal temperature signature in the isotherms above 960 mb is also noteworthy.

The dewpoint cross-section, Fig 37, also shows the moist surface layer increasing with time between 27/0000Z and 27/1300Z and nearly constant between 27/1300Z and 27/2300Z. At 950 mb on 27/0700Z, another distinct moist pocket is depicted. The refractive layer is also present on the 27th (Figs 38 and 39) centered at approximately 980 mb.

c. 28 August 1993

The diurnal pattern of the potential temperature timesection (Fig. 36) on the 26th and 27th continues. The inversion lowers between 28/0000Z and 28/0600Z, rises between 28/0600Z and 28/1600Z and remains steady between 28/1600Z and 29/0000Z. The inversion has weakened and becomes more diffuse than on earlier days.

As the inversion drops and the moisture levels decrease from 28/0000Z to 28/0500Z, Figs 38 and 39 show that the trapping layer also falls and extends to the surface on 28/0500Z. The trapping layer then rises and is reestablished at 28/2000Z at 960 mb. Another distinct dry pocket is depicted at 965 mb on 28/0400Z.

2. GB-HIS Measurements

a. 26 August 1993

The GB-HIS potential temperature timesection (Fig. 40) depicts the low-level inversion, or stable layer from 980 mb to 955 mb at 26/0349Z. This inversion shows the same diurnal oscillation of the observed inversion but is weaker. Above 950 mb between 26/1100Z and 27/0000Z, the rapid rise and fall of the theta surfaces represents the passage of a stratus overcast that adversely affected the data at 26/1200Z. The GB-HIS dewpoint temperature timesection (Fig. 41) also captures the diurnal signature below 950 mb with the moist

surface layer rising between 26/0000Z and 26/1200Z and falling between 26/1200Z and 27/0000Z. The pronounced moistening at 875 mb on 26/1200Z is erroneous and to the passage of the stratus overcast.

Figures 42 and 43 show the presence of a trapping layer at 955 mb between 26/0400Z and 26/2000Z. The presence of this refractive layer is due to the inversion and the rapid decrease in moisture from 975 mb to 950 mb between 26/1200Z and 26/1800Z. The observed data shows that the trapping layer is actually lower since the moist layer is shallower in the raob data.

b. 27 August 1993

Although the inversion is weaker than observed, the GB-HIS does capture the diurnal signature of the marine inversion (Fig 40). Above 950 mb, the diurnal heating pattern that exists at lower levels is present although the atmosphere is less stable. The GB-HIS (Fig 41) indicates a diurnal pattern in the moist near-surface layer and other moisture details as depicted in Fig 37. Once again, GB-HIS data, Figs 42 and 43, shows a trapping layer present from the surface to 980 mb between 27/0000Z and 28/0000Z where a rapid decrease in moisture occurs. The observed data shows a broad moist region from the surface to 980 mb above which the refractive layer is located. The GB-HIS refractive layer analyses is very close to observed conditions for the second half of the 27th.

c. 28 August 1993

Figure 40 shows the persistent diurnal signature in the marine inversion continuing through the 28th. The moist surface layer depicted in Fig 41 continues to show the diurnal pattern that has been present throughout the three day period although a drying of the air above the moist surface layer is present at 950 mb. The GB-HIS shows trapping at 980 mb between 28/0600Z and 28/2300Z (Figs 42 and 43) associated with the rapid decrease in moisture from the surface to 950 mb and the inversion. Raob data shows this trapping layer to be slightly higher at 960 mb on 28/2000Z.

3. Summary

The PTMUGU 1993 data illustrated that the GB-HIS is also skillful in describing the diurnal patterns that occur within the marine boundary layer as well as the periodic temperature changes that occur above the low level marine inversion. The depiction of the evolution of the low level marine is a positive result of these evaluation experiments.

The GB-HIS analyzed refractive conditions were reasonable for the second half of the 27th and the 28th. However, the GB-HIS results continue to miss small scale moisture features and the accurate description of the vertical moisture structure within the lower troposphere. Consequently, the refractivity timesections were adversely

affected and incorrectly depicted in position, location and time.

V. CONCLUSIONS

An assessment on military applications of the GB-HIS retrievals was conducted from the over water PTSUR 1991 and 1992 cruises and the shoreline 1993 VOCAR (PTMUGU). Comparisons of GB-HIS retrievals with radiosonde data, revealed strengths and weaknesses in the GB-HIS ability to measure the marine boundary layer.

The strengths of the GB-HIS are its ability to measure the thermal structure of the marine boundary layer and monitor the changes in the low-level inversion that caps the marine boundary layer. Strengths were illustrated in each experimental period. The PTSUR 1991 data showed the dramatic lifting of the inversion during the frontal passage and captured the development of the deep, well-mixed boundary layer as well. During the PTSUR 1992 cruise, the land-breeze induced inversion change near the end of the cruise is well depicted by the GB-HIS. Finally, the PTMUGU 1993 GB-HIS data resolved the diurnal oscillations of a coastal boundary layer.

The primary weakness of the GB-HIS is its inability to resolve the observed detailed moisture structure of the coastal boundary layer. Although the general larger scale vertical moisture gradient was present in the retrievals, all of the narrow moist and dry zones during the experimental period were not resolved. These difficulties in moisture

retrieval had a considerably adverse affect on the monitoring of refractive trapping layers in the three data sets.

Determining sharp vertical moisture gradients are critical to measuring refractivity. Specifically, the M and dM/dZ timesections from the PTSUR 1991 GB-HIS results describe the initial location and time of the trapping layer, at 08/00Z. However, the GB-HIS did not detect the moistening that occurred prior to the frontal passage. Hence, GB-HIS refractive timesections depicts the trapping layer to be longer in duration. The PTSUR 1992 GB-HIS M and dM/dZ timesections did not accurately depict the refractive layers that were present. This was due to the poor depiction of the intense dry zone that occurred between 09/16Z and 10/00Z in the dewpoint timesection. Finally, the PTMUGU 1993 dewpoint timesections shows that the inconsistencies in depicting the intense dry layer present at 26/0400Z and 28/0400Z and the moistening that occurred at 950 mb on 27/0600Z is the major cause for the inconsistency in depicting the refractive layers. The conclusion from the three experimental data sets is the GB-HIS estimates of refraction are poor.

Hourly data was found not useful because of the excessive noise in the data. The amplitude of the noise prevented the accurate depiction of any high frequency meteorological features that may have been present in the data.

The results of this military assessment are that 1) the GB-HIS is effective in measuring marine temperature inversions

inversions and the marine boundary layer evolution, 2) the GB-HIS can measure large scale features and trends in moisture but is not effective in measuring small scale moisture features and 3) due to the moisture retrieval problem, the GB-HIS may not be useful in measuring refractivity in a coastal regime.

Recommendations for further study are: 1) to determine the effect on retrieval accuracy of using the new universal coefficients for the GB-HIS processing on PTSUR 1991 and PTSUR 1992 data, 2) to determine the effect of marine aerosols on retrieval accuracy, and 3) militarily assess the evolution of refractivity in a coastal regime using other remote sensor systems such as LIDAR, that also participated in VOCAR.

APPENDIX

This appendix serves as a convenient location to consolidate all the figures discussed in the text of this thesis.

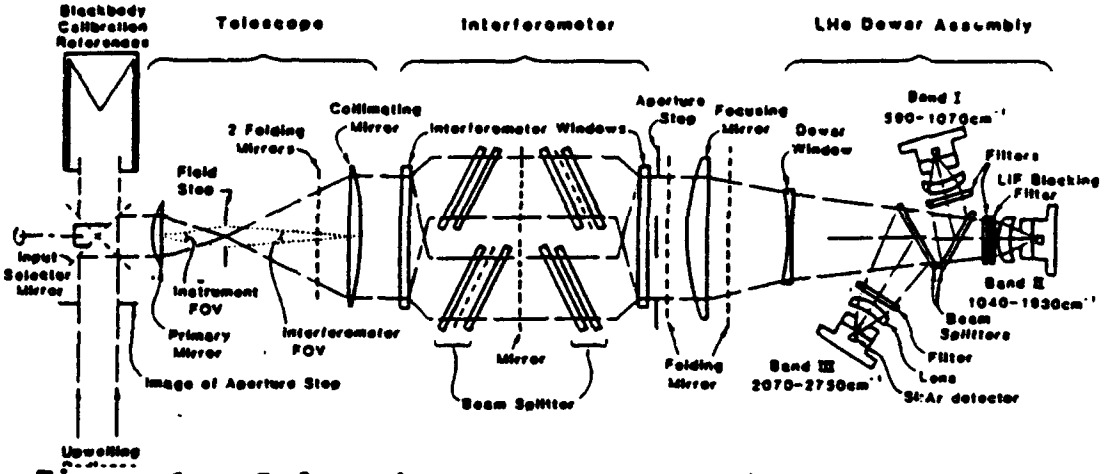

Figure 1: Infrared spectrum over which the HIS samples its data as seen from a space-based instrument.

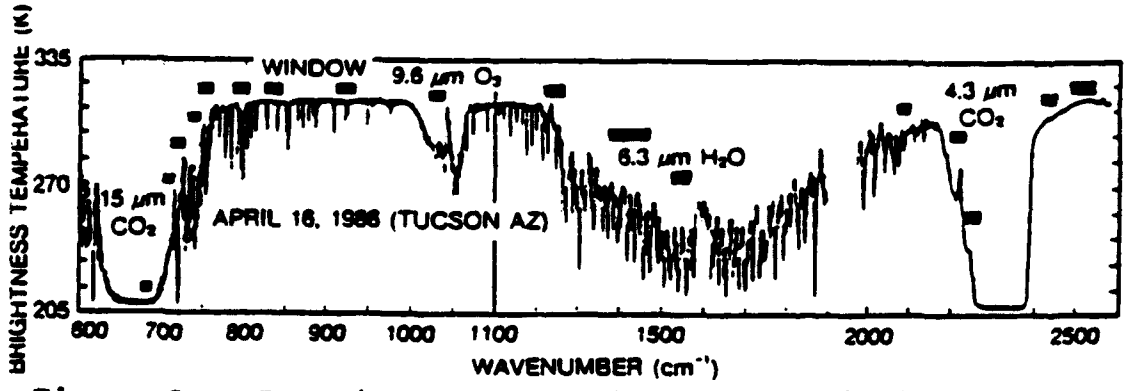

Figure 2: Functional schematic of a typical 3-channel Michelson interferometer. (Revercomb et al. 1988)

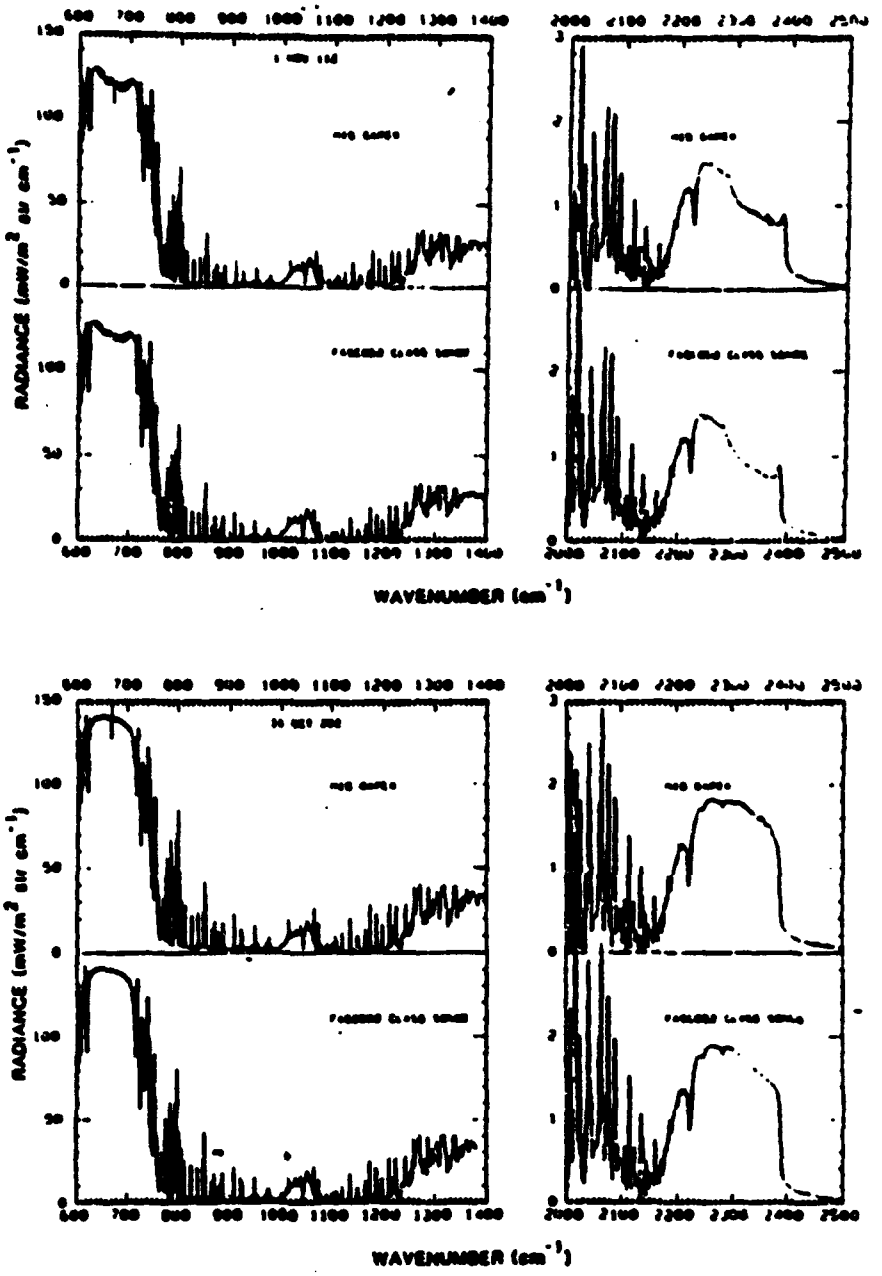

Figure 3: Two examples of comparisons between downwelling radiance spectra observed by the HIS and calculated using a CLASS temperature and water-vapor sounding. (Smith et al., 1990)

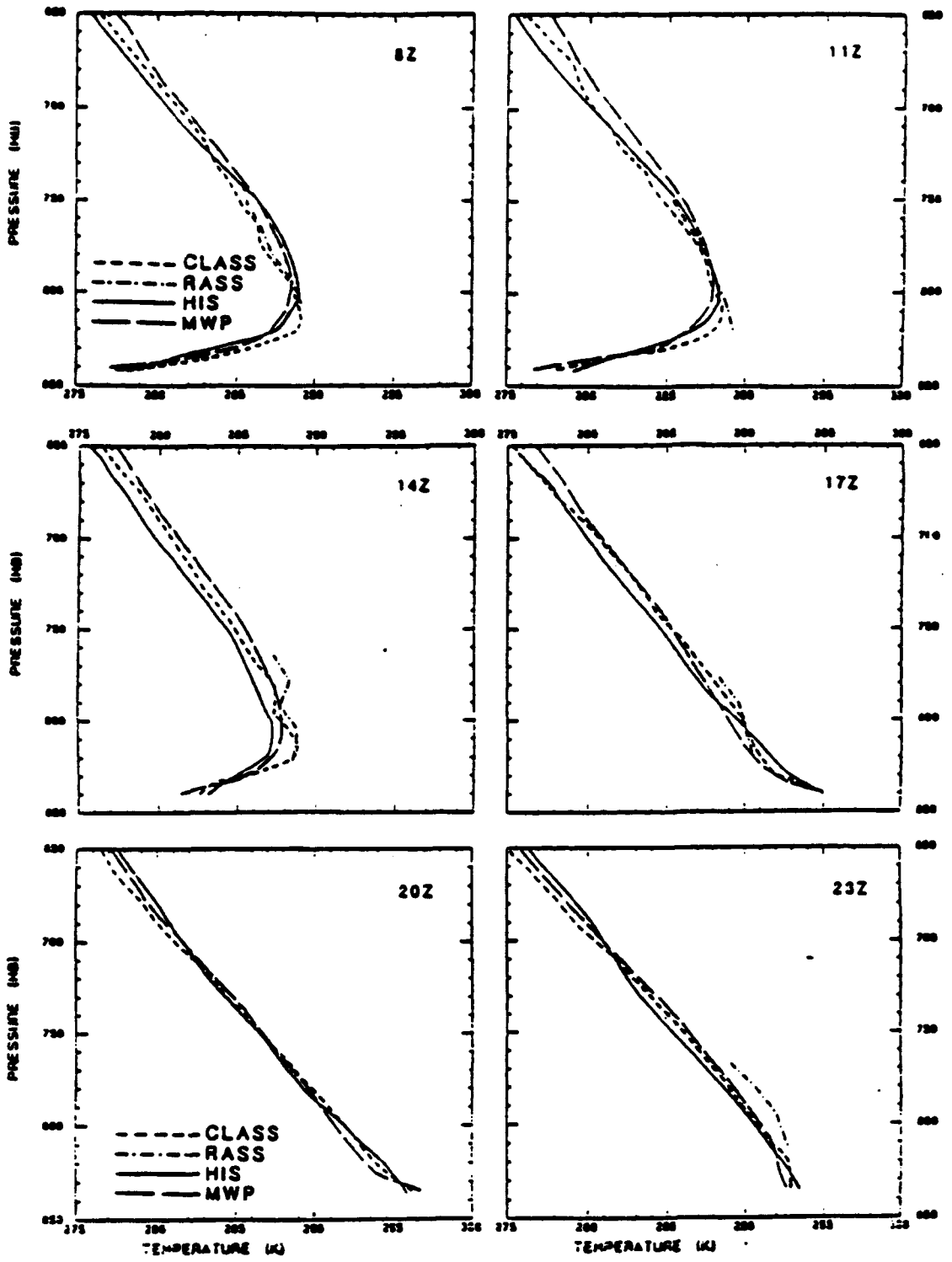

Figure 4: Temperature profiles observed by CLASS, RASS, HIS, and MWP sounding systems. (Smith et al., 1990)

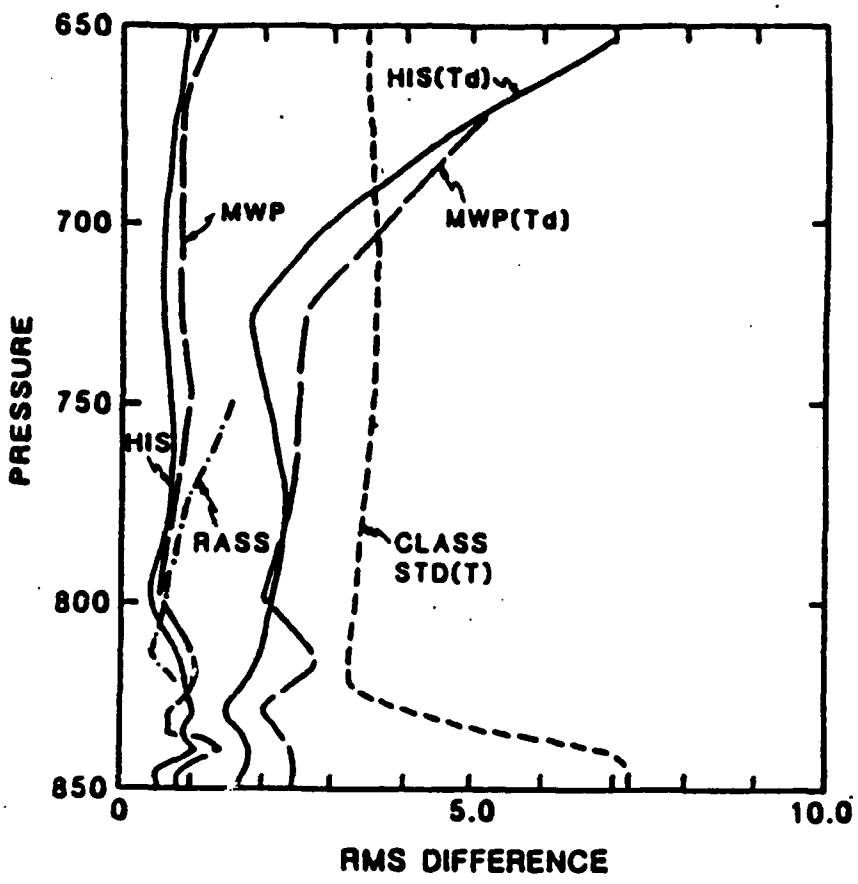

Figure 5: RMS difference between three remote sensing systems from the CLASS observations. (Smith et al., 1990)

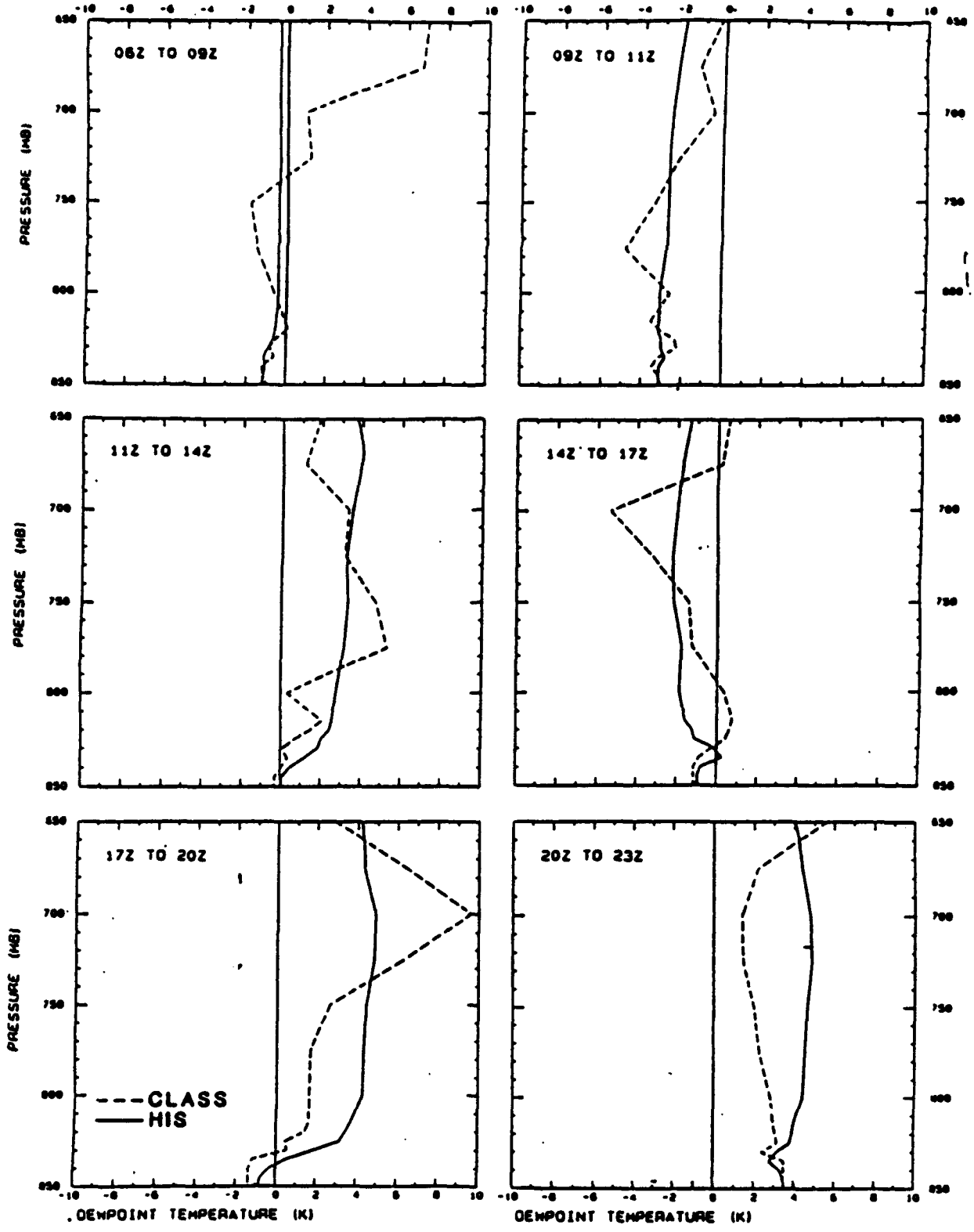

Figure 6: 3 hour time tendency of dewpoint temperature profiles by the HIS and CLASS sounding systems on 1 November 1988. (Smith et al., 1990)

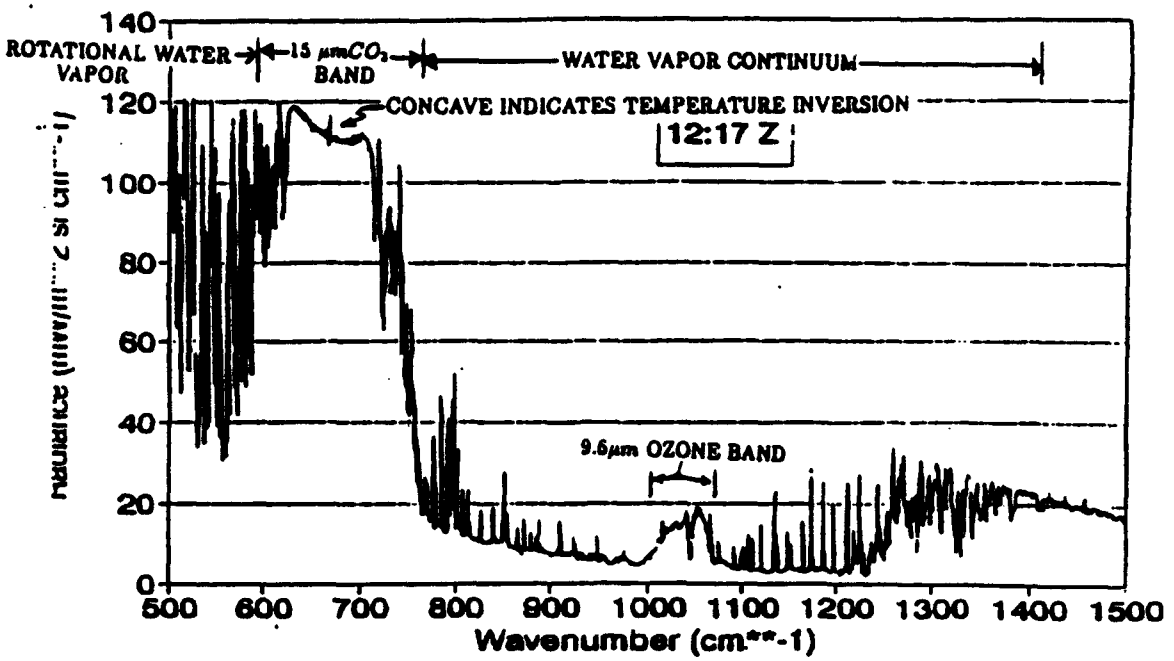

Figure 7: GB-HIS radiance spectra observed on 28 February 1991 at 1217Z in Denver, Colorado (INVERSION).

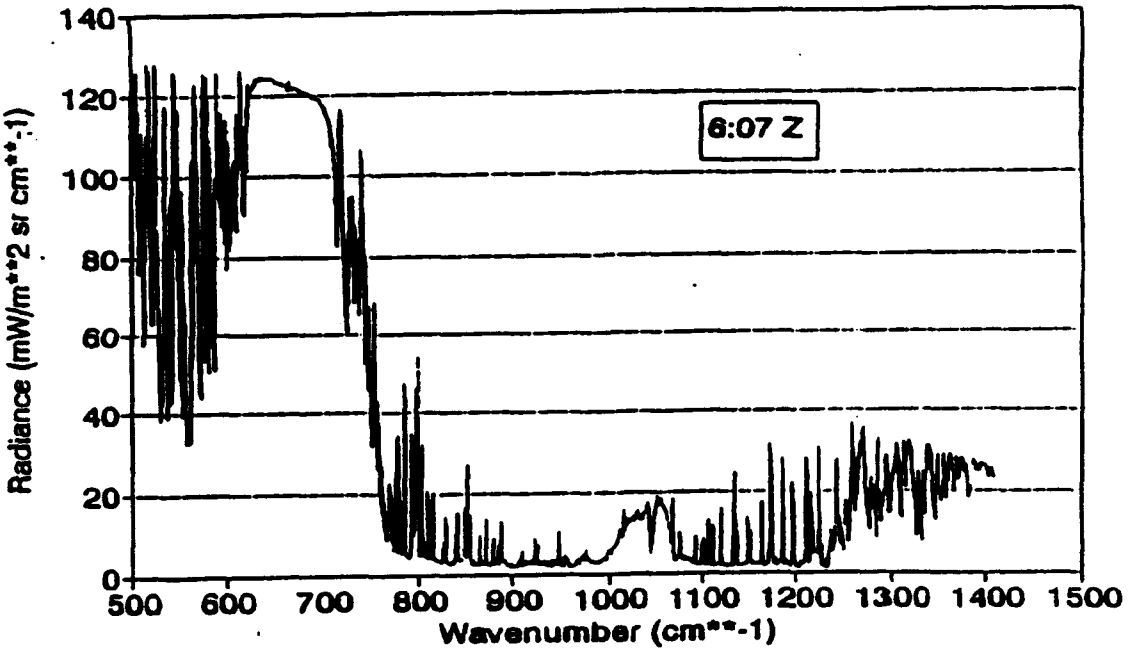

Figure 8: GB-HIS radiance spectra observed on 28 February 1991 at 0607Z in Denver, Colorado (NO INVERSION).

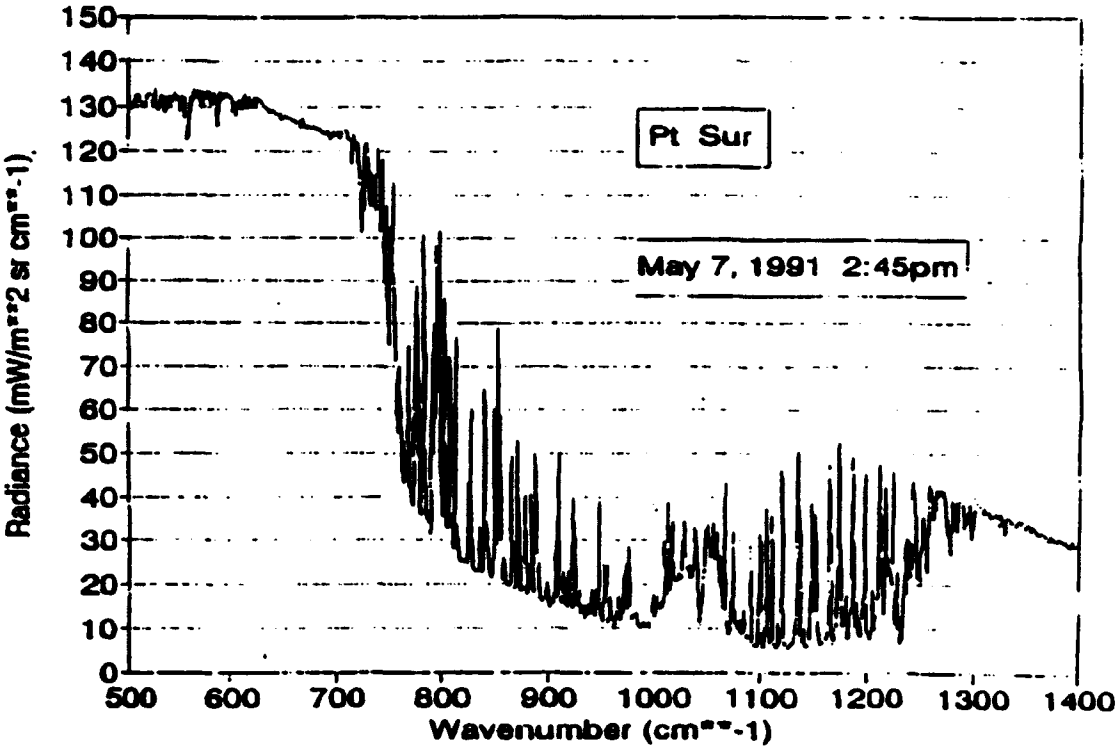

Figure 9: GB-HIS radiance spectra observed on 7 May 1991 at 1445 local time during the PTSUR 1991 cruise (INVERSION).

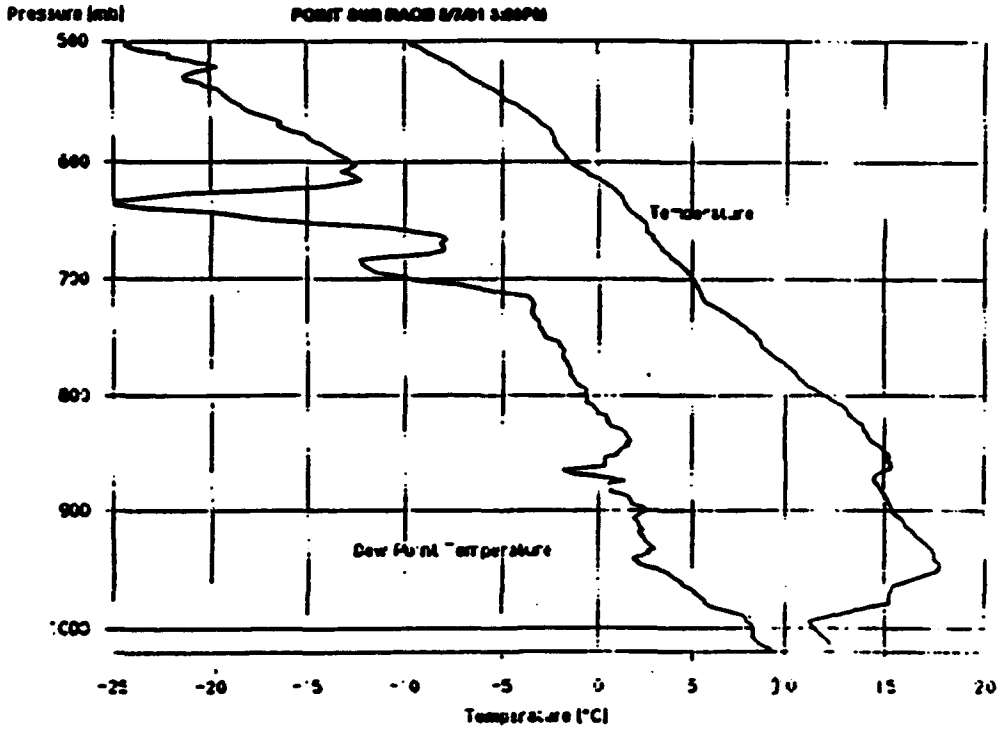

Figure 10: Radiosonde observation on 7 May 1991 at 1500 local time during the PTSUR 1991 cruise (INVERSION).

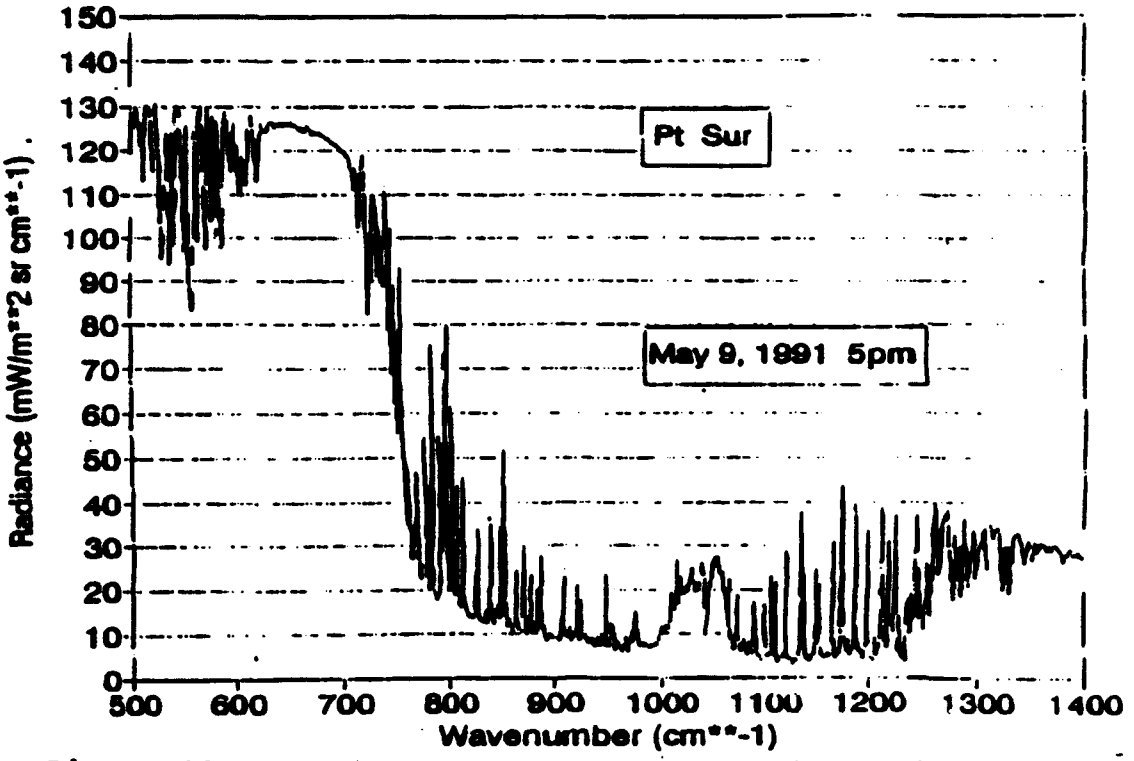

Figure 11: GB-HIS radiance spectra observed on 9 May 1991 at 1700 local time during the PTSUR 1991 cruise (NO INVERSION).

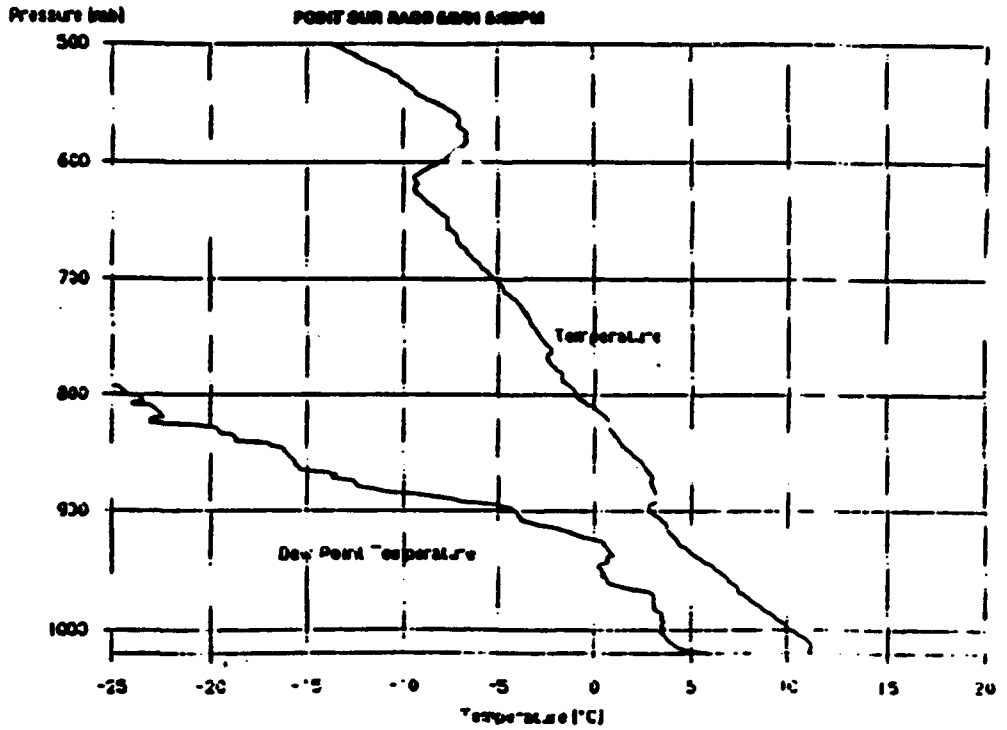

Figure 12: Radiosonde observation on 9 May 1991 at 1700 local time during the PTSUR 1991 cruise (NO INVERSION).

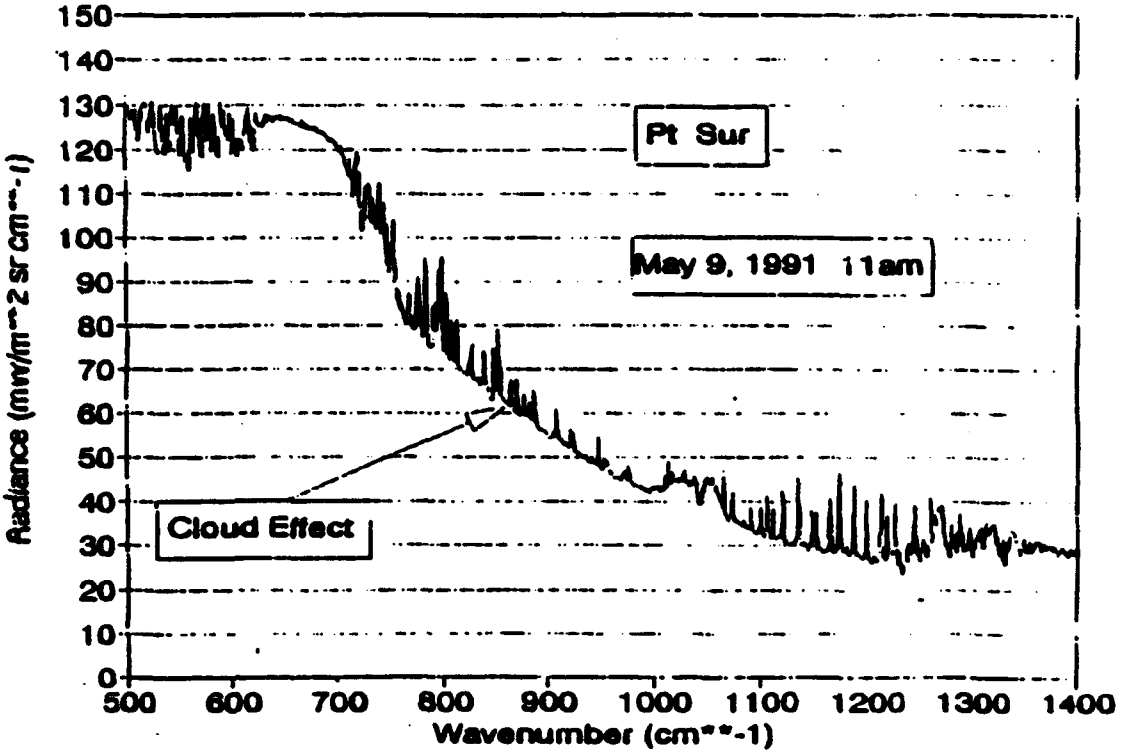

Figure 13: GB-HIS radiance spectra observed on 9 May 1991 at 1100 local time during the PTSUR 1991 cruise (LOW CLOUDS).

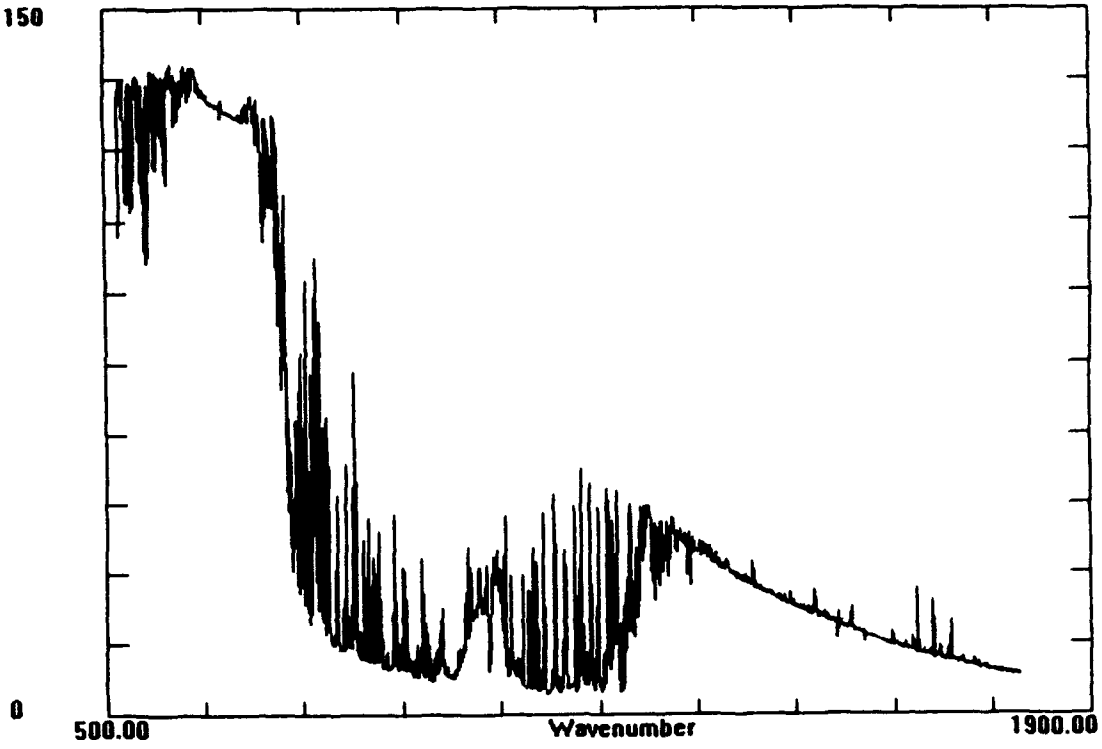

Figure 14a: GB-HIS radiance spectra observed on 10 May 1992 at 0257Z during the PTSUR 1992 cruise.

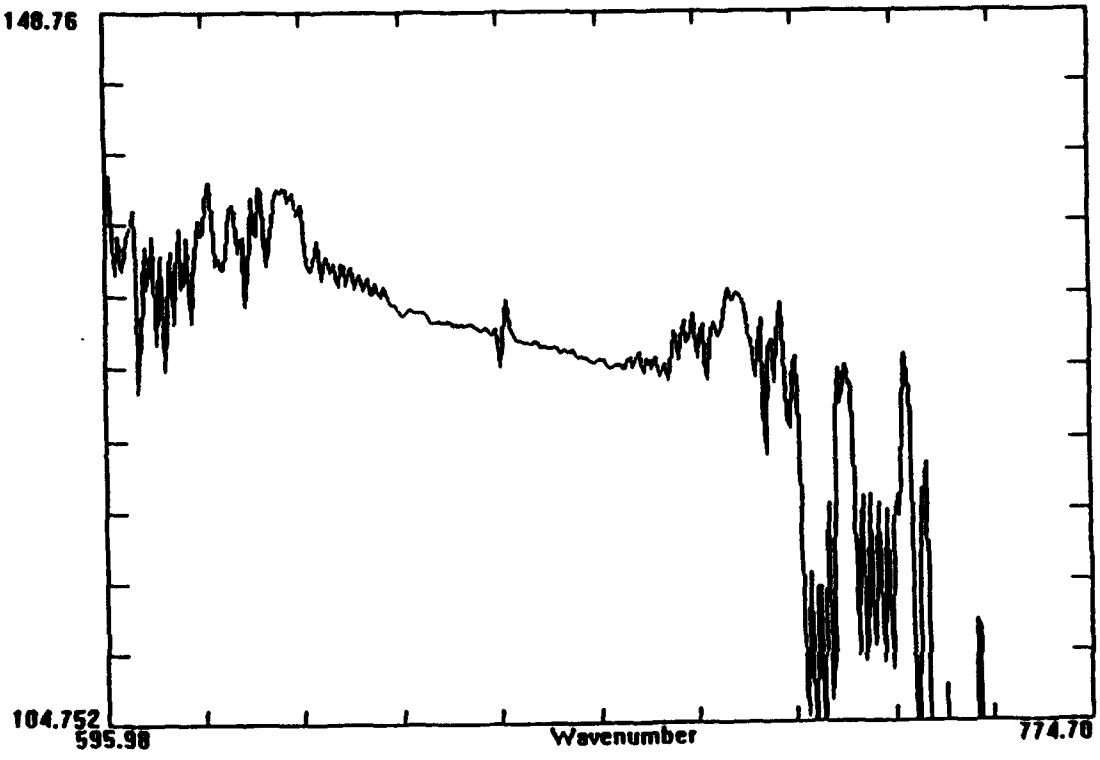

Figure 14b: Blow-up of the 15 μm CO_2 band from the GB-HIS radiance spectra on 10 May 1992 at 0257Z.

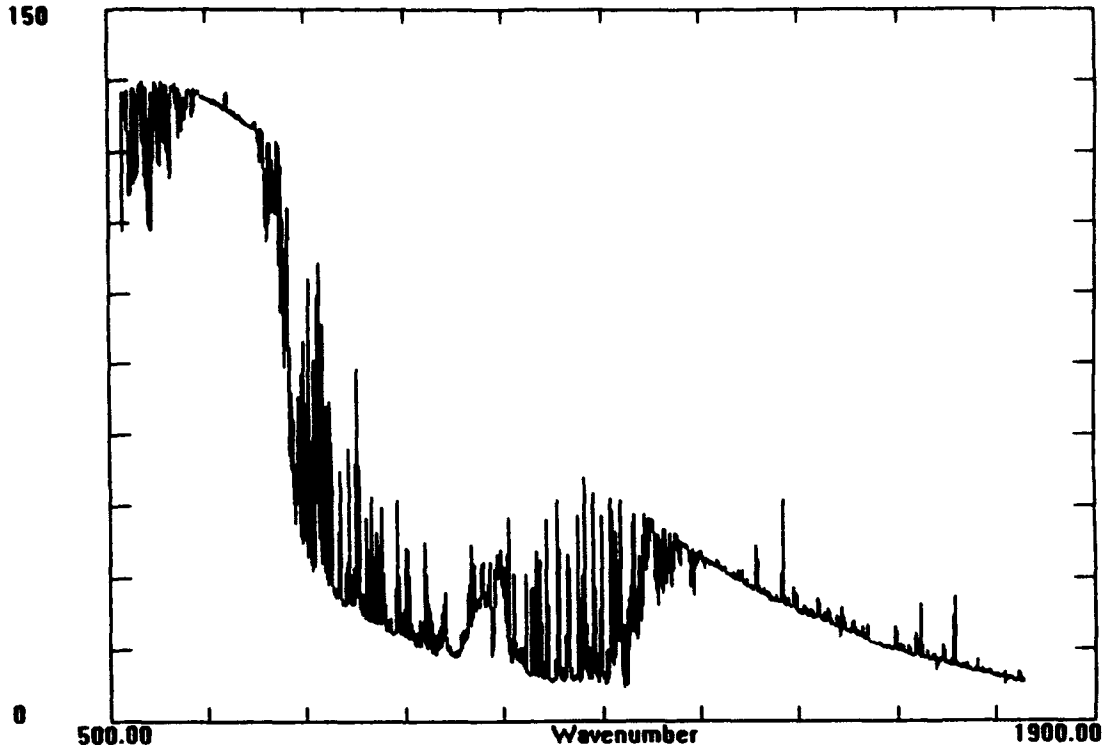

Figure 15: GB-HIS radiance spectra observed on 10 May 1992 at 0000Z during the PTSUR 1992 cruise.

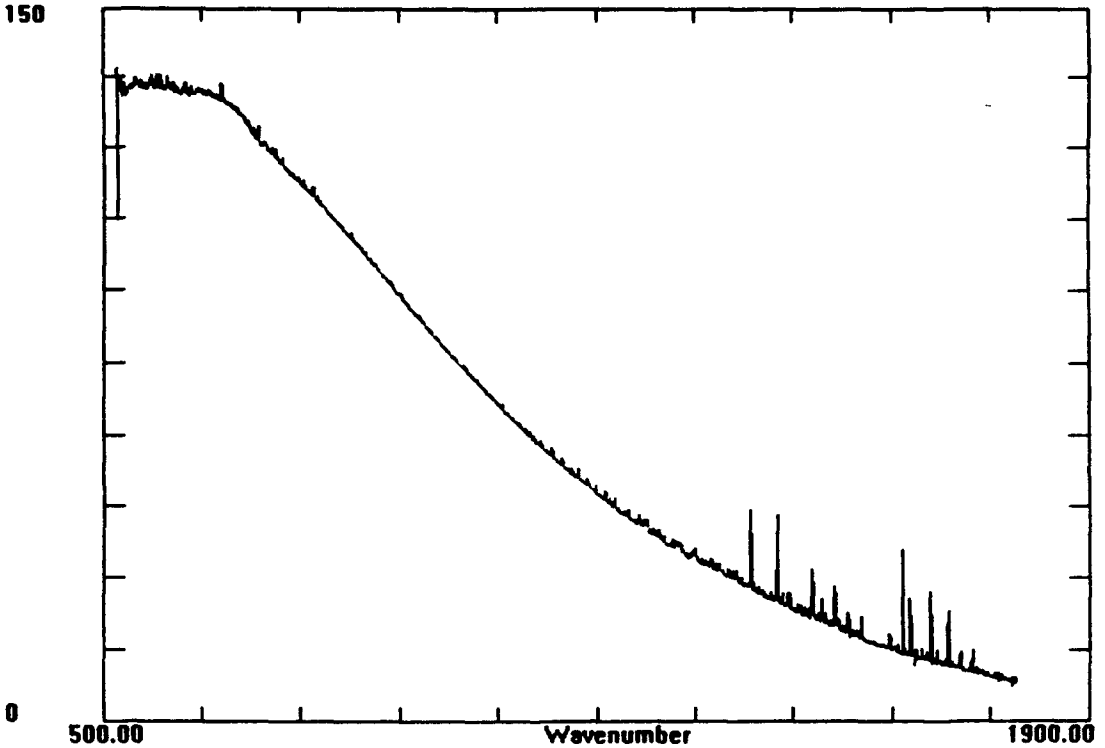

Figure 16: GB-HIS radiance spectra observed on 10 May 1992 at 1700Z during the PTSUR 1992 cruise (STRATUS OVERCAST).

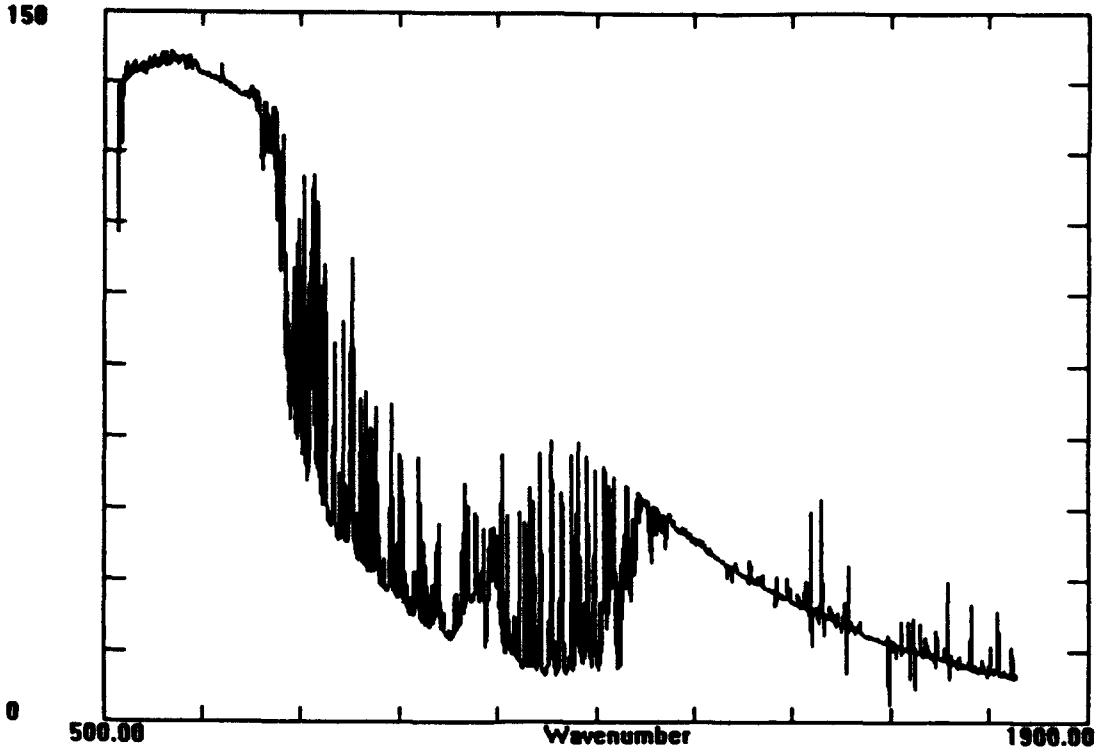

Figure 17: GB-HIS radiance spectra observed on 26 August 1993 at 0400Z during the VOCAR experiment in Point Mugu.

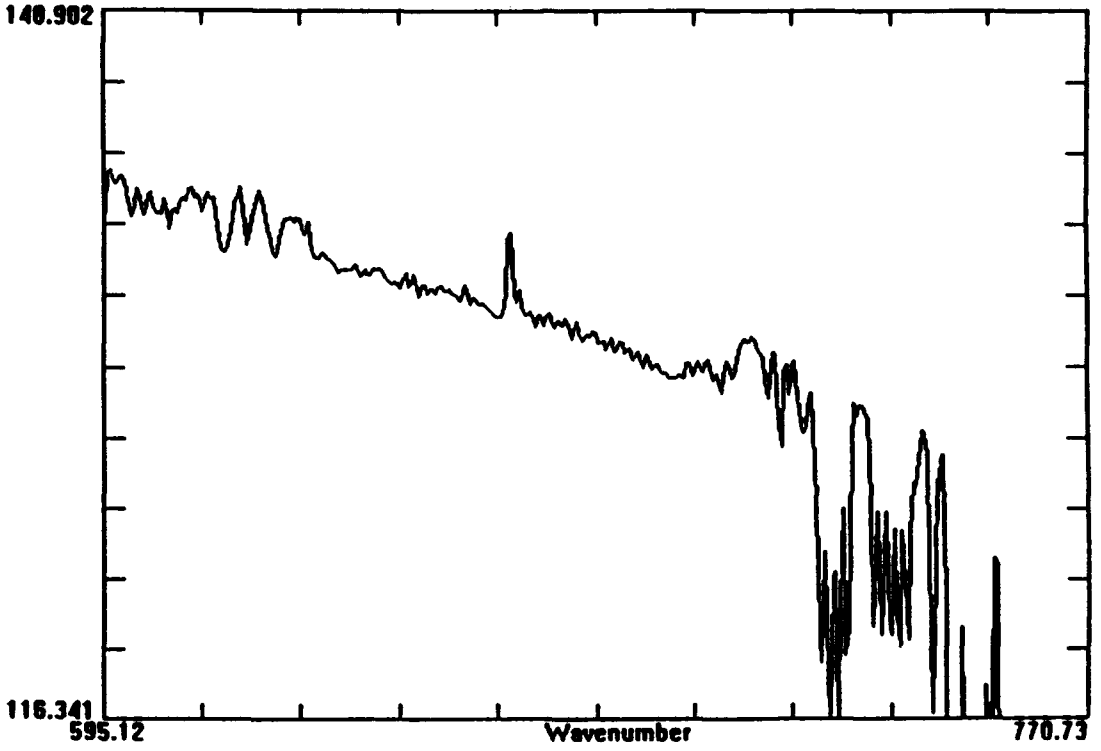

Figure 18: Blow-up of the 15 μm CO_2 band from the GB-HIS radiance spectra observed on 26 August 1993 at 0400Z.

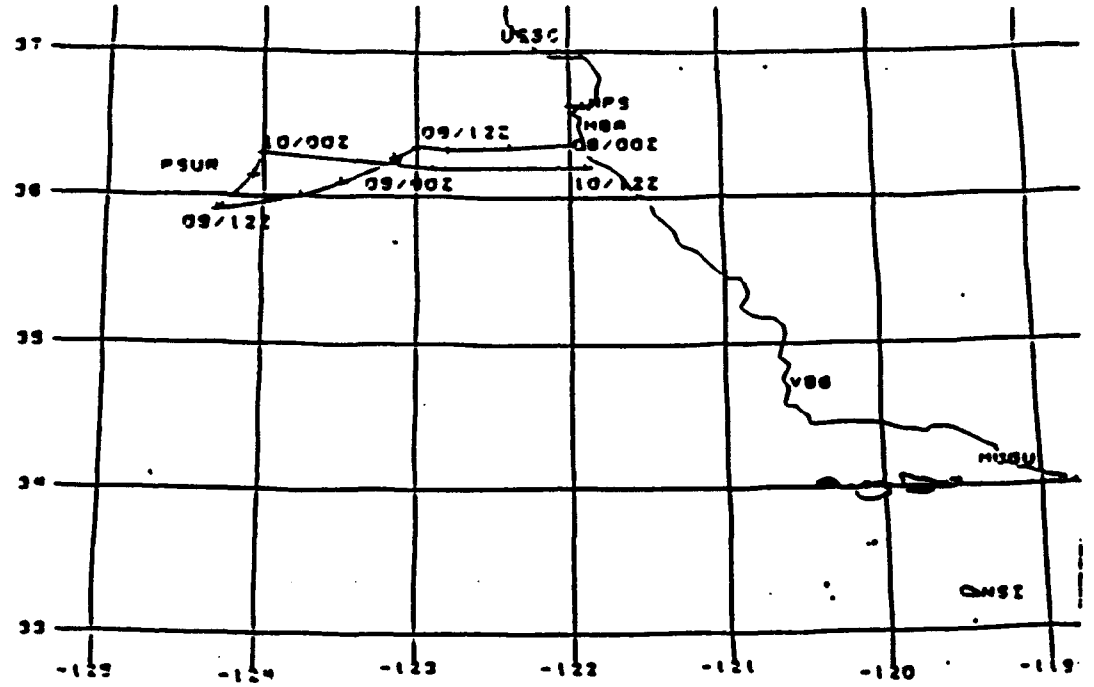

Figure 19a: Ship track for the PTSUR 1991 cruise.

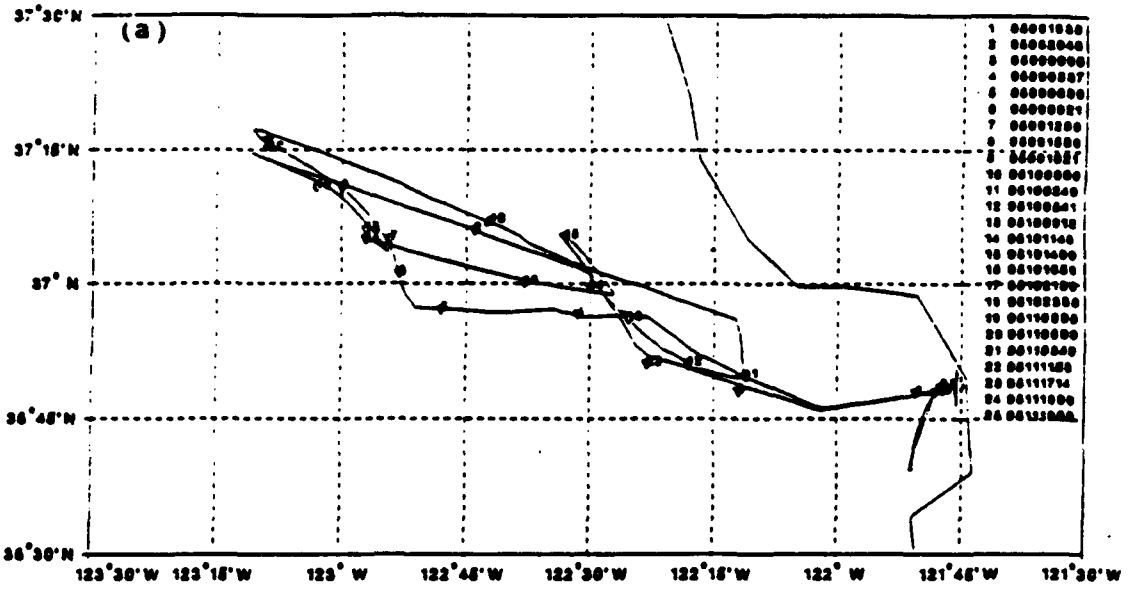

Figure 19b: Ship track for the PTSUR 1992 cruise.

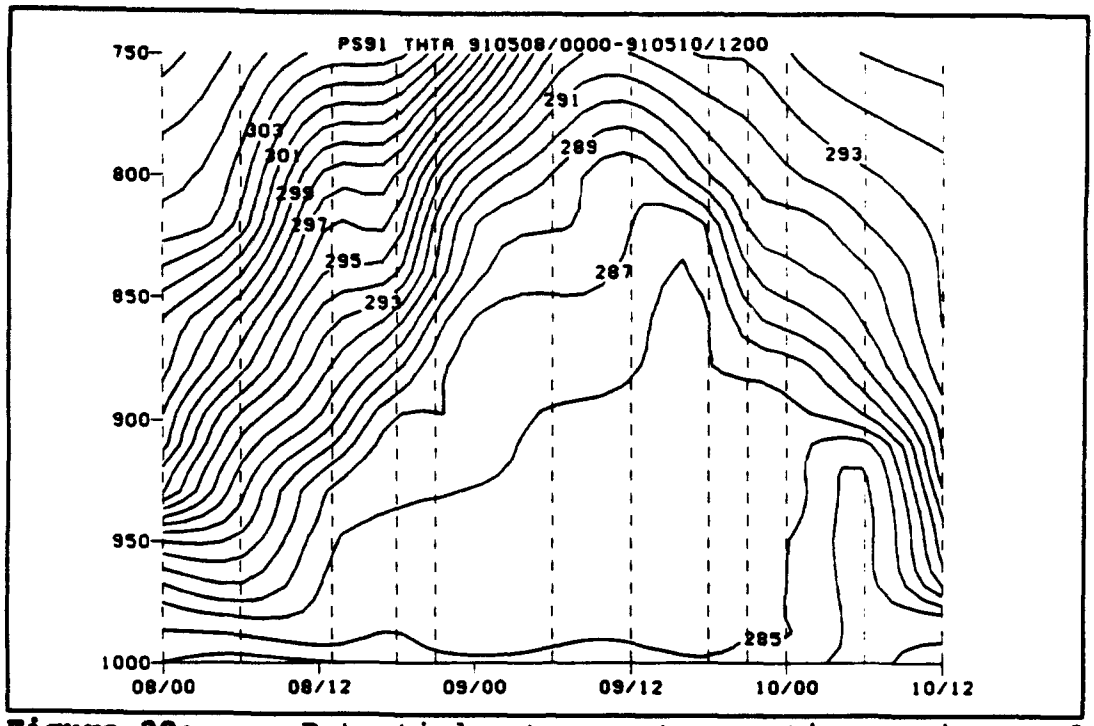

Figure 20: Potential temperature timesection of radiosonde observations from 8-10 May 1991 during the PTSUR 1991 cruise.

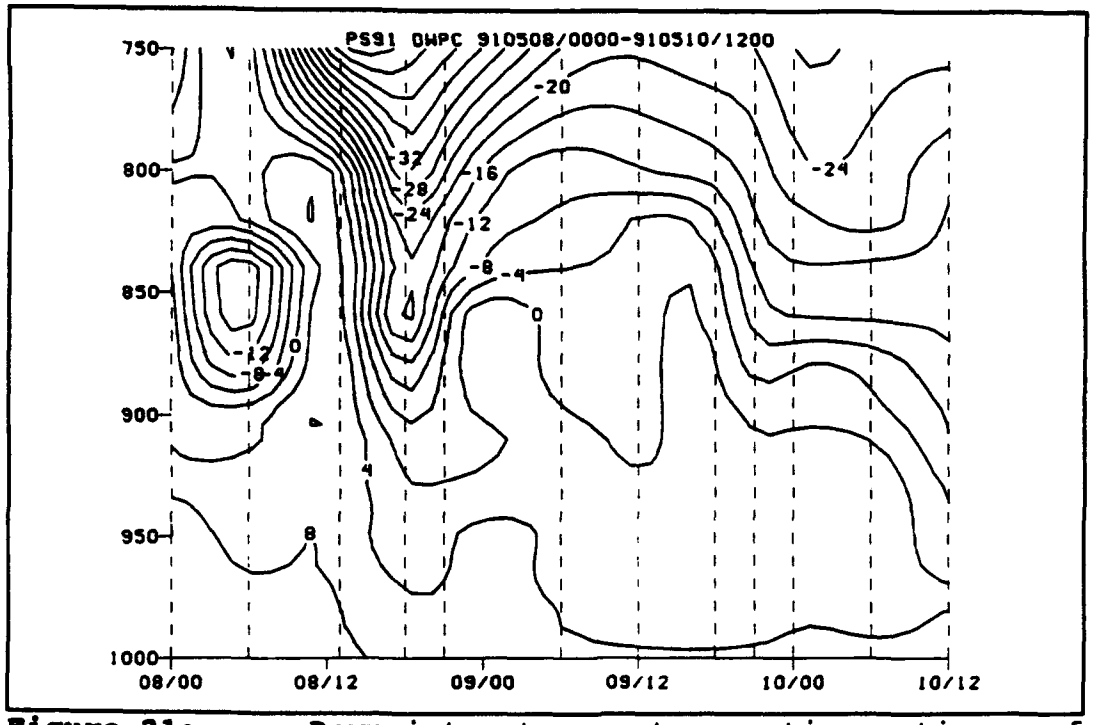

Figure 21: Dewpoint temperature timesection of radiosonde observations from 8-10 May 1991 during the PTSUR 1991 cruise.

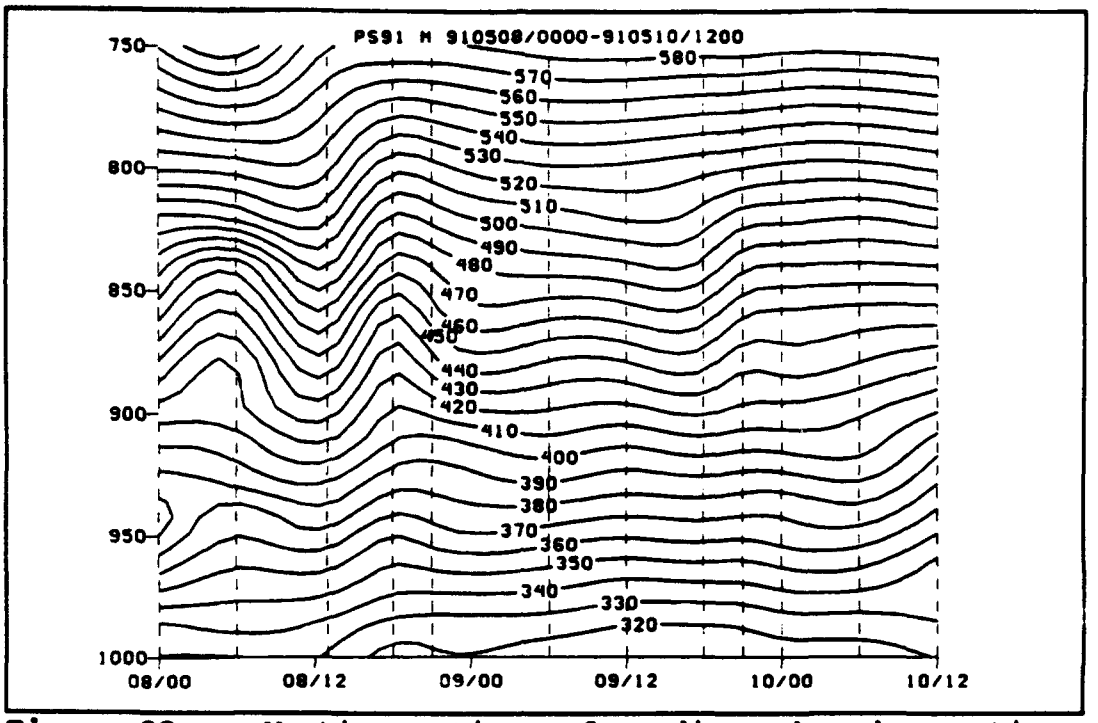

Figure 22: M timesection of radiosonde observations from 8-10 May 1991 during the PTSUR 1991 cruise.

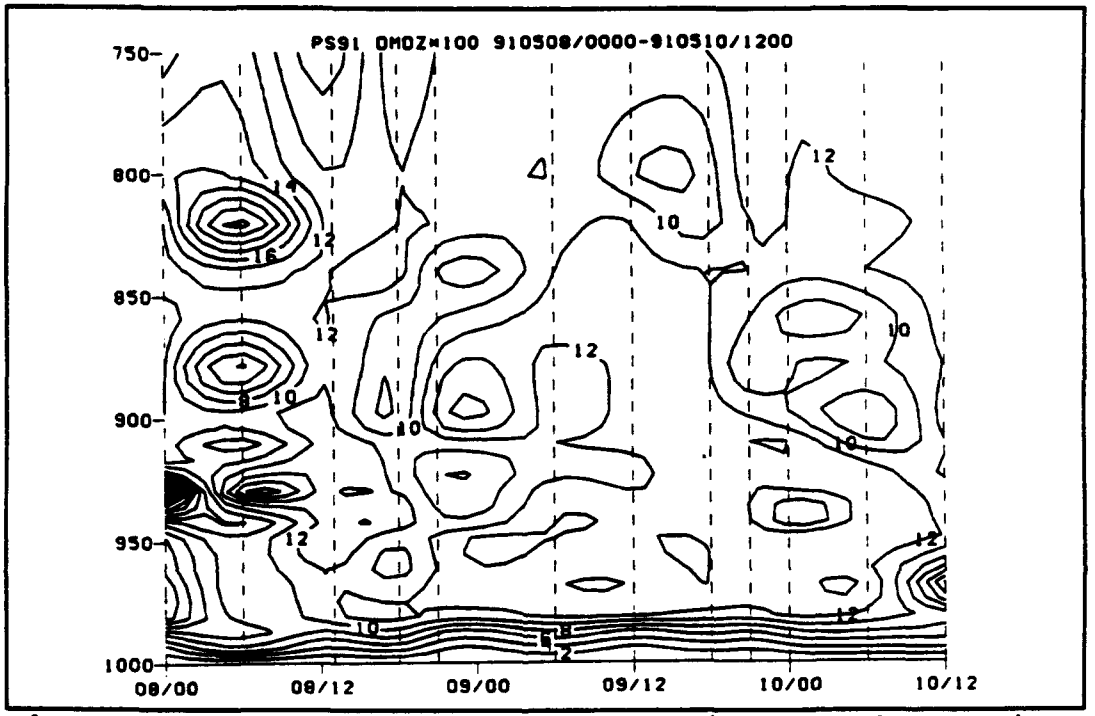

Figure 23: dM/dZ timesection of radiosonde observations from 8-10 May 1991 during the PTSUR 1991 cruise.

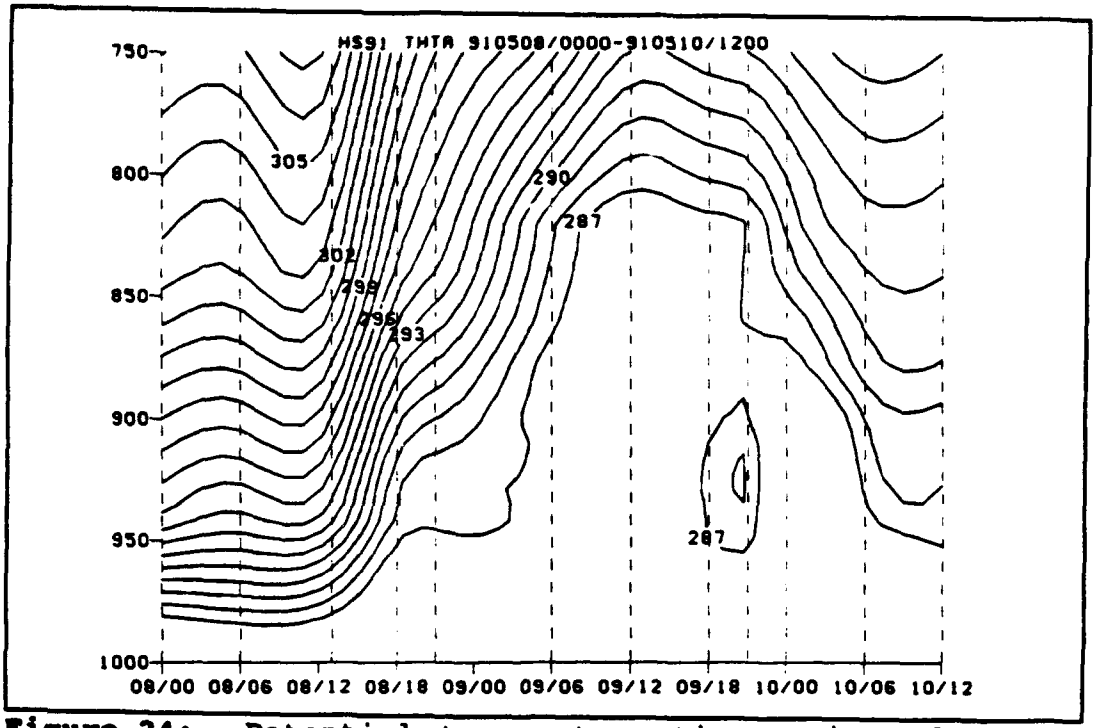

Figure 24: Potential temperature timesection of GB-HIS measurements from 8-10 May 1991 during the PTSUR 1991 cruise.

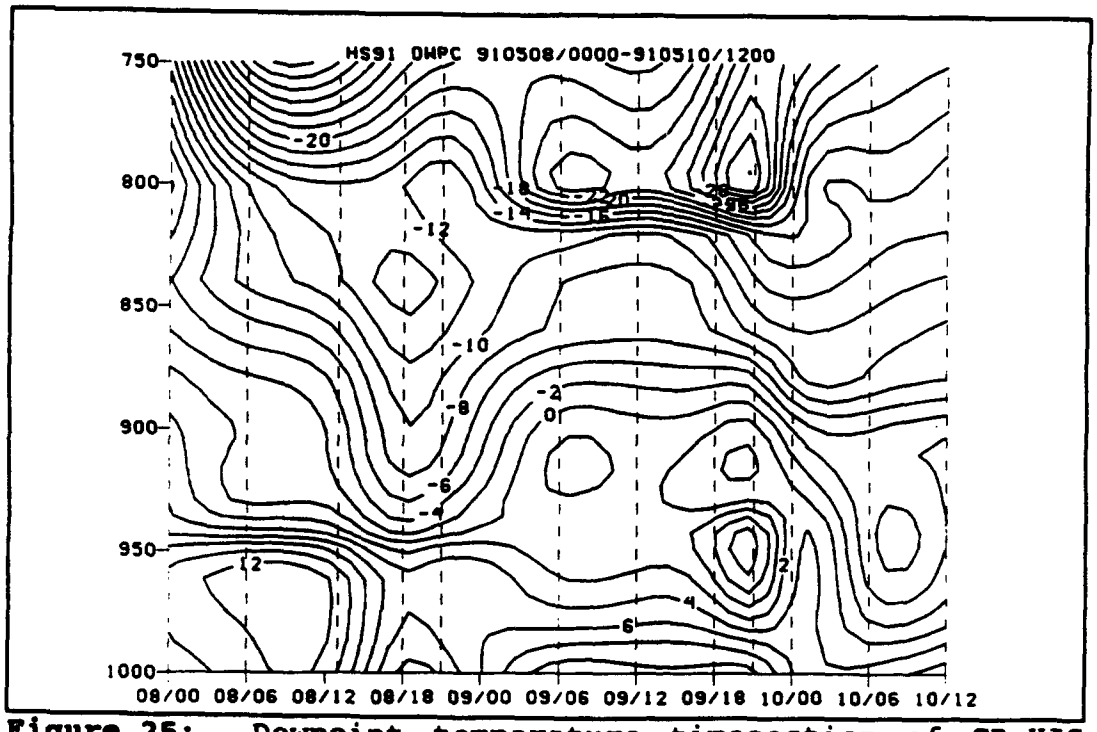

Figure 25: Dewpoint temperature timesection of GB-HIS measurements from 8-10 May 1991 during the PTSUR 1991 cruise.

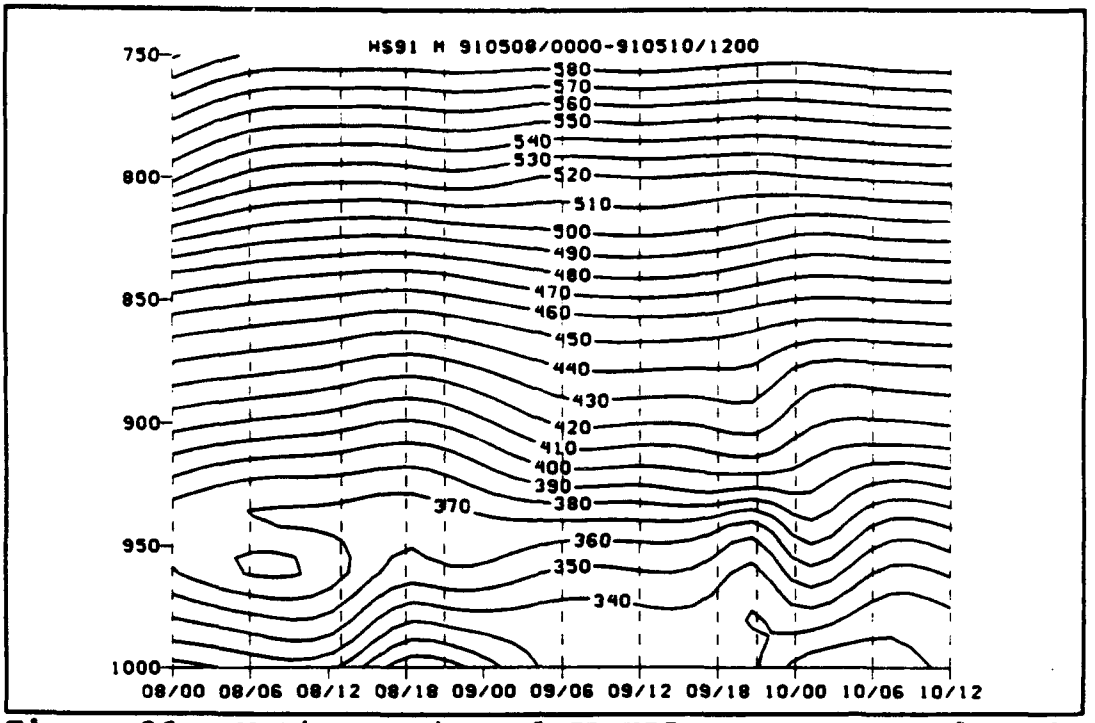

Figure 26: M timesection of GB-HIS measurements from 8-10 May 1991 during the PTSUR 1991 cruise.

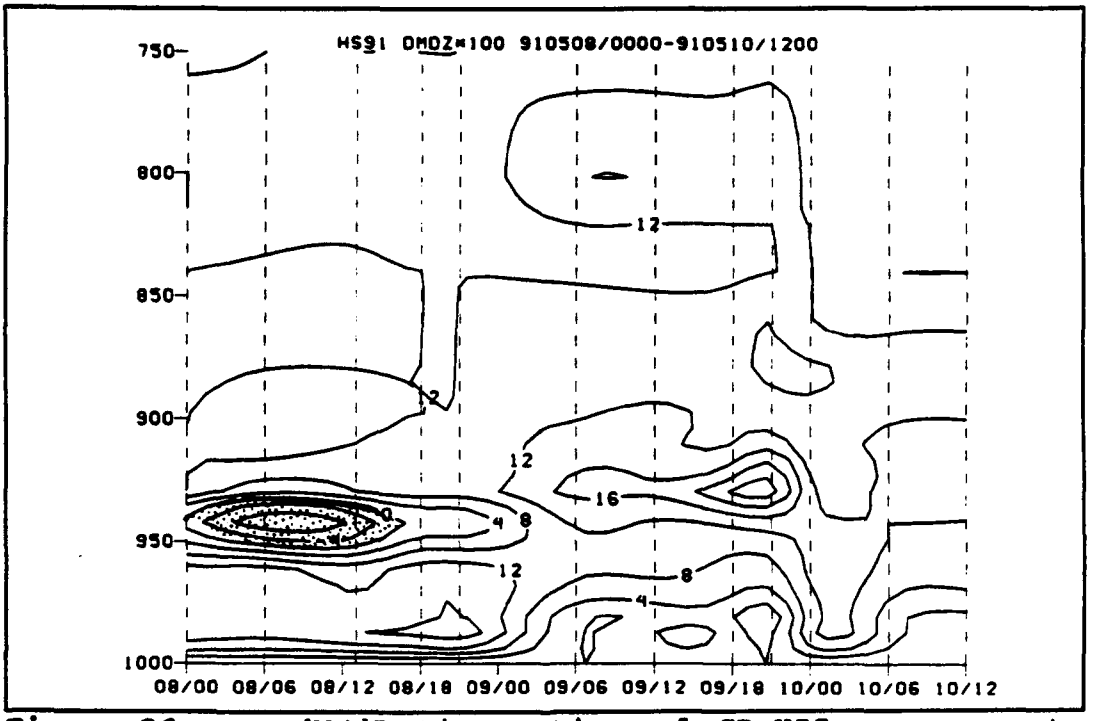

Figure 26a: dM/dZ timesection of GB-HIS measurements from 8-10 May 1991 during the PTSUR 1991 cruise.

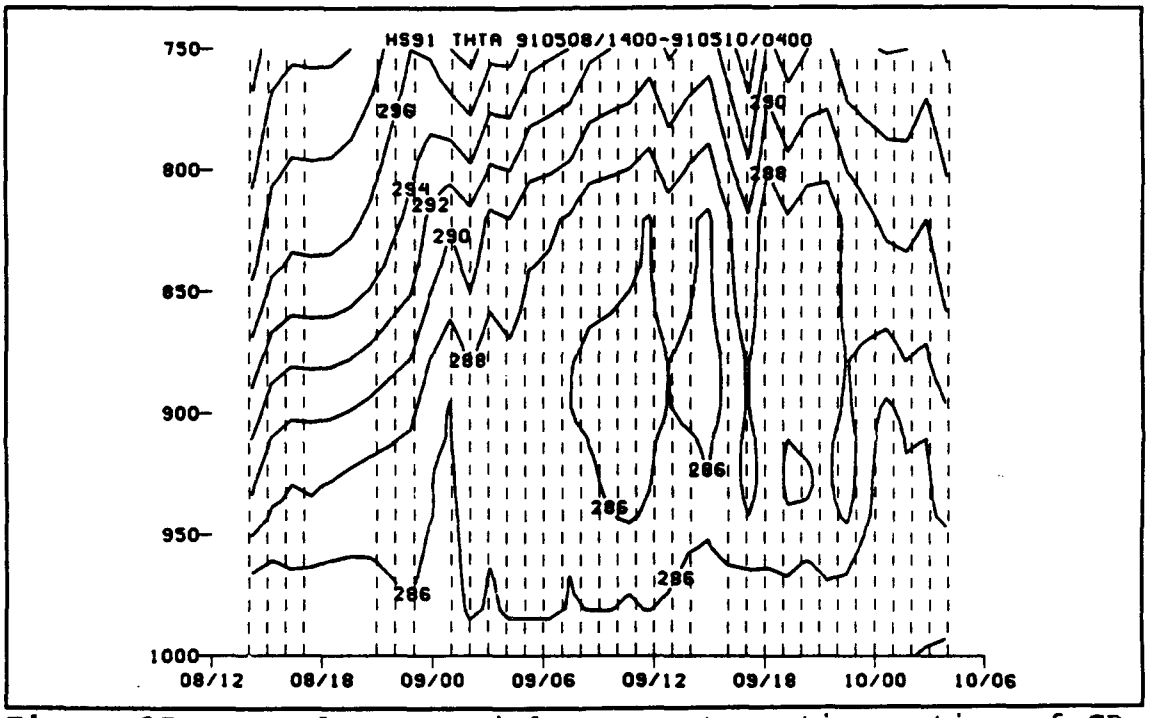

Figure 27: Hourly potential temperature timesection of GB-HIS measurements from 8-10 May 1991 during the PTSUR 1991 cruise.

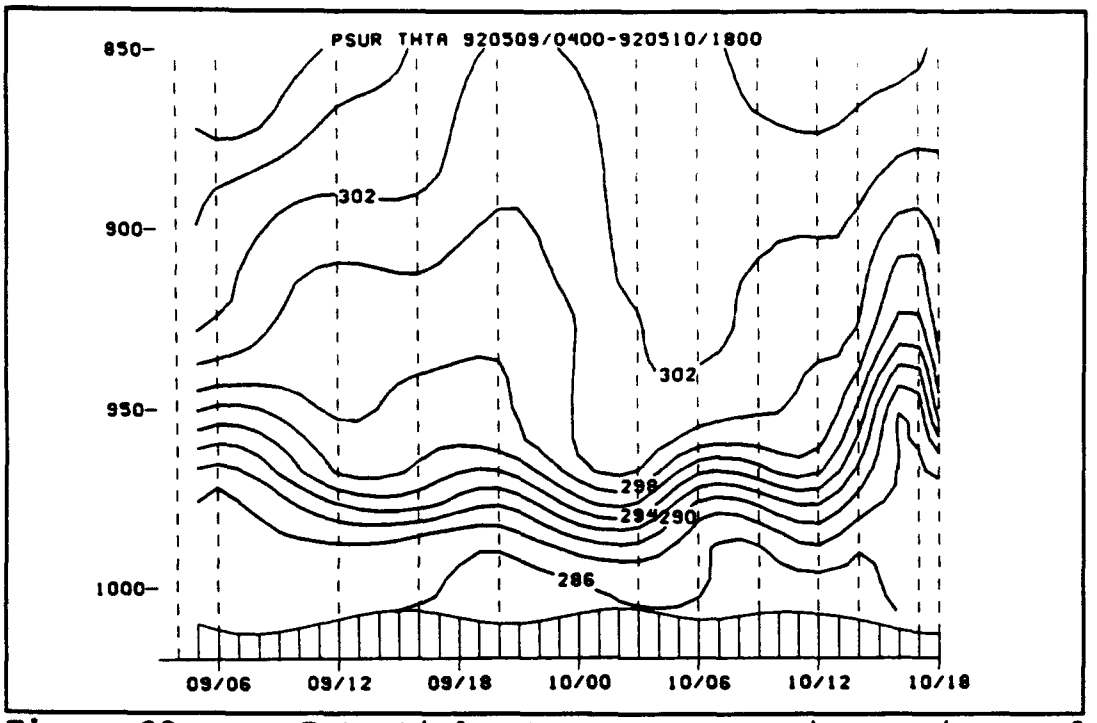

Figure 28: Potential temperature timesection of radiosonde observations from 9-10 May 1992 during the PTSUR 1992 cruise.

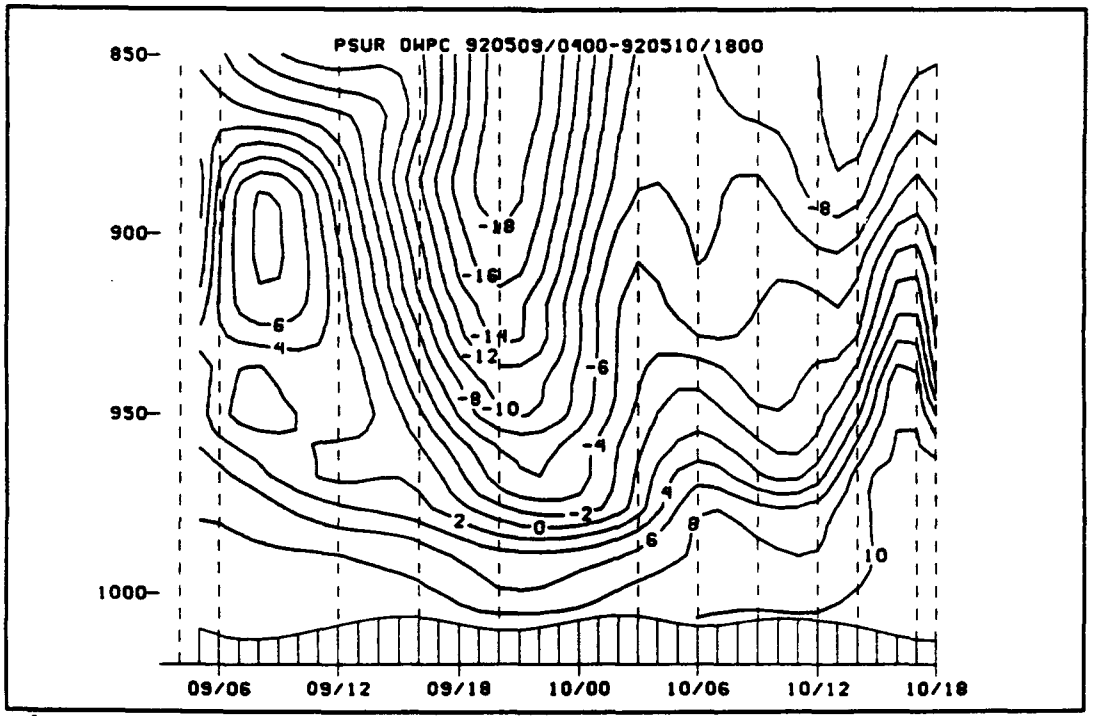

Figure 29: Dewpoint temperature timesection of radiosonde observations from 9-10 May 1992 during the PTSUR 1992 cruise.

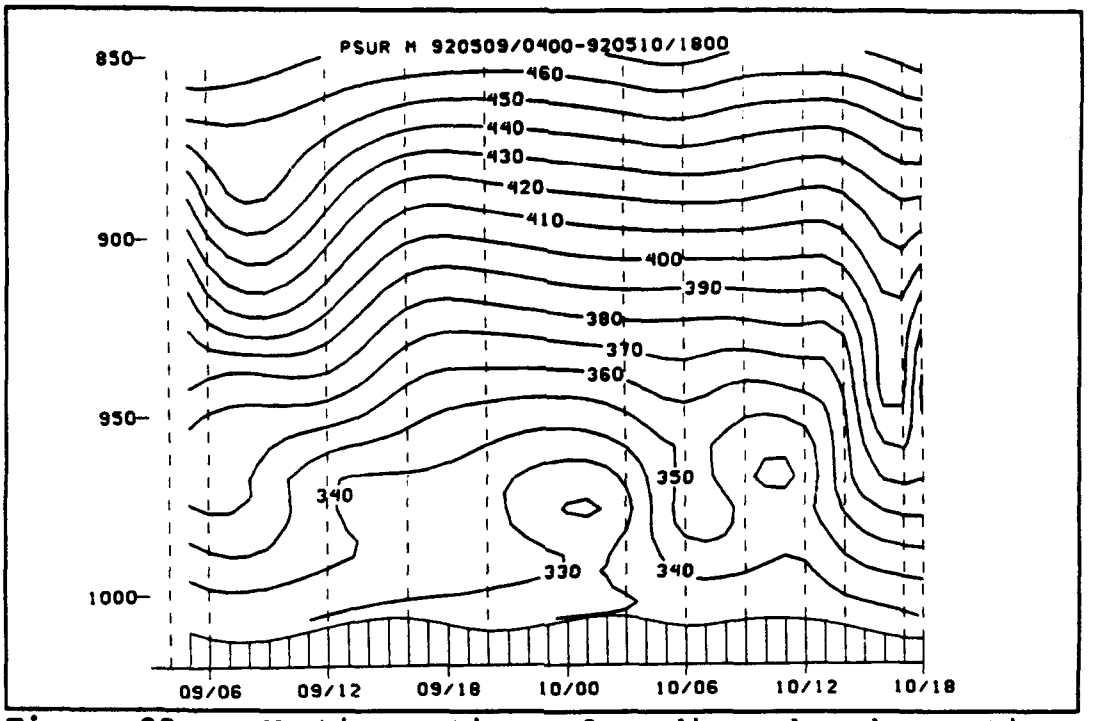

Figure 30: M timesection of radiosonde observations from 9-10 May 1992 during the PTSUR 1992 cruise.

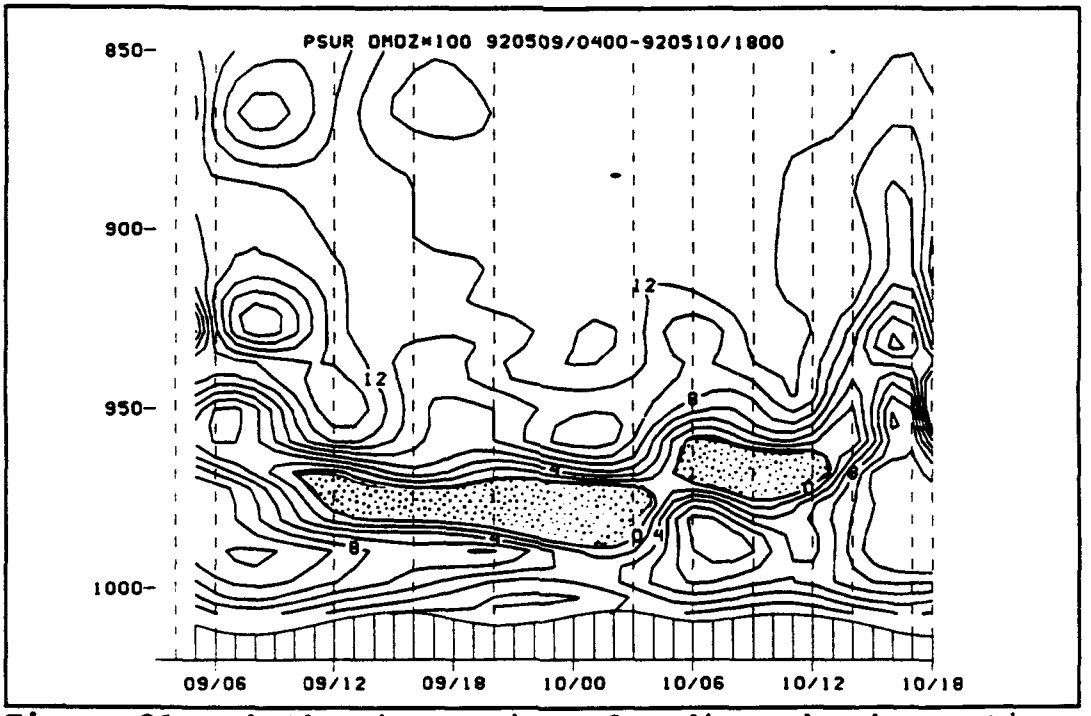

Figure 31: dM/dZ timesection of radiosonde observations from 9-10 May 1992 during the PTSUR 1992 cruise.

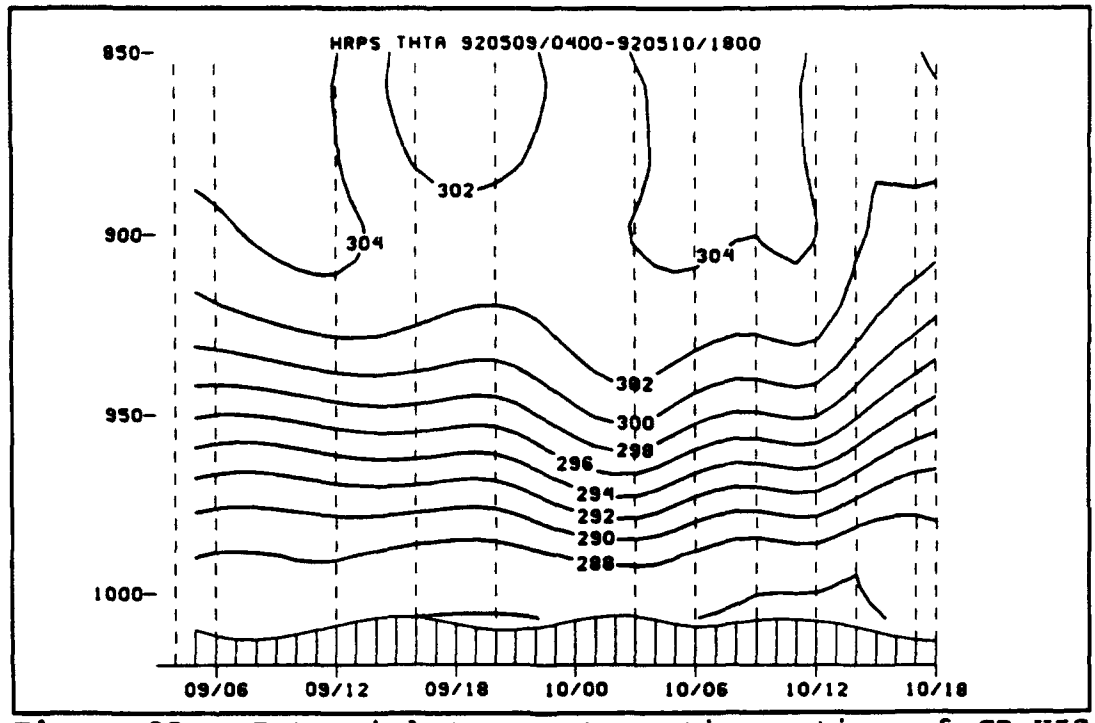

Figure 32: Potential temperature timesection of GB-HIS measurements from 9-10 May 1992 during the PTSUR 1992 cruise.

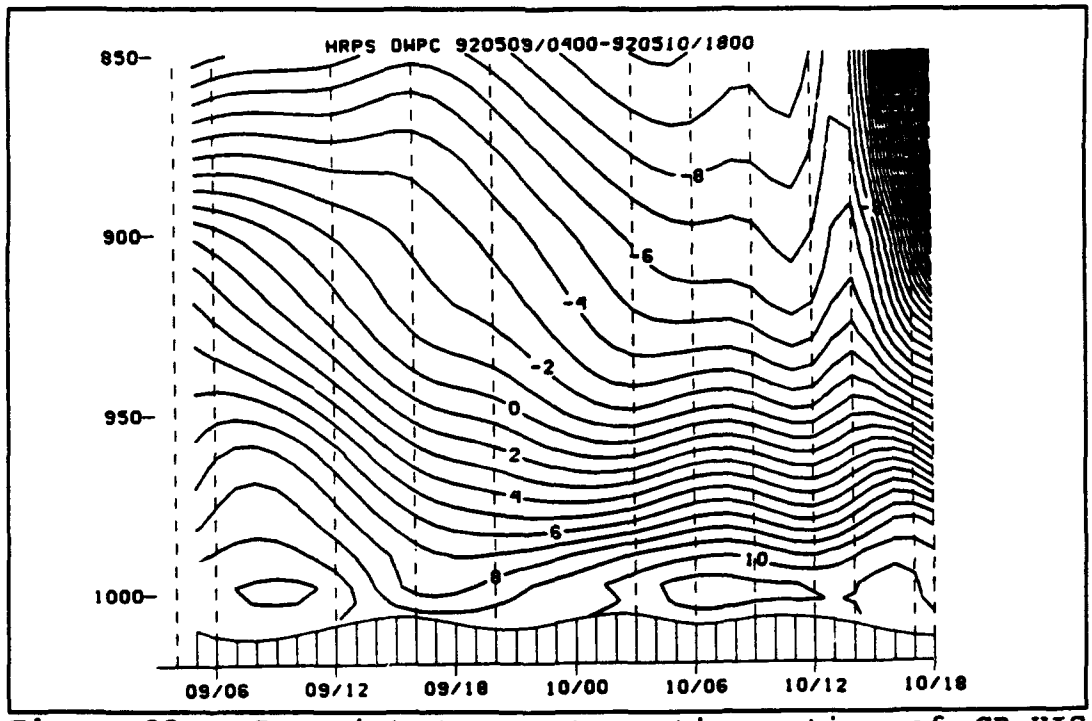

Figure 33: Dewpoint temperature timesection of GB-HIS measurements from 9-10 May 1992 during the PTSUR 1992 cruise.

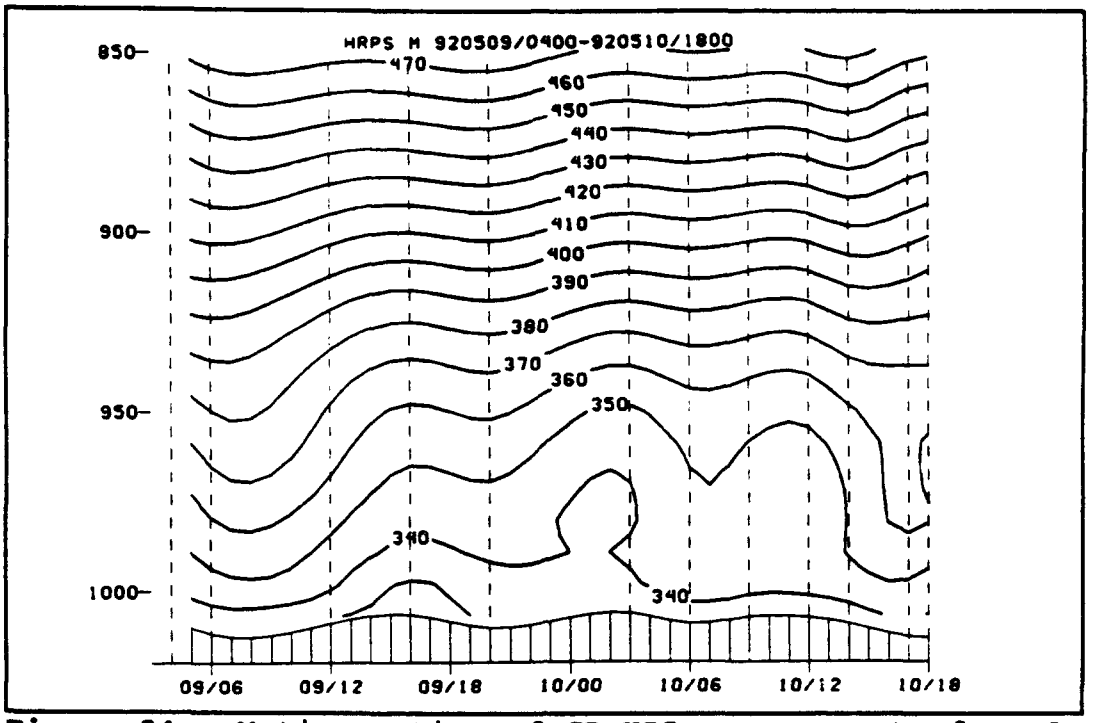

Figure 34: M timesection of GB-HIS measurements from 9-10 May 1992 during the PTSUR 1992 cruise.

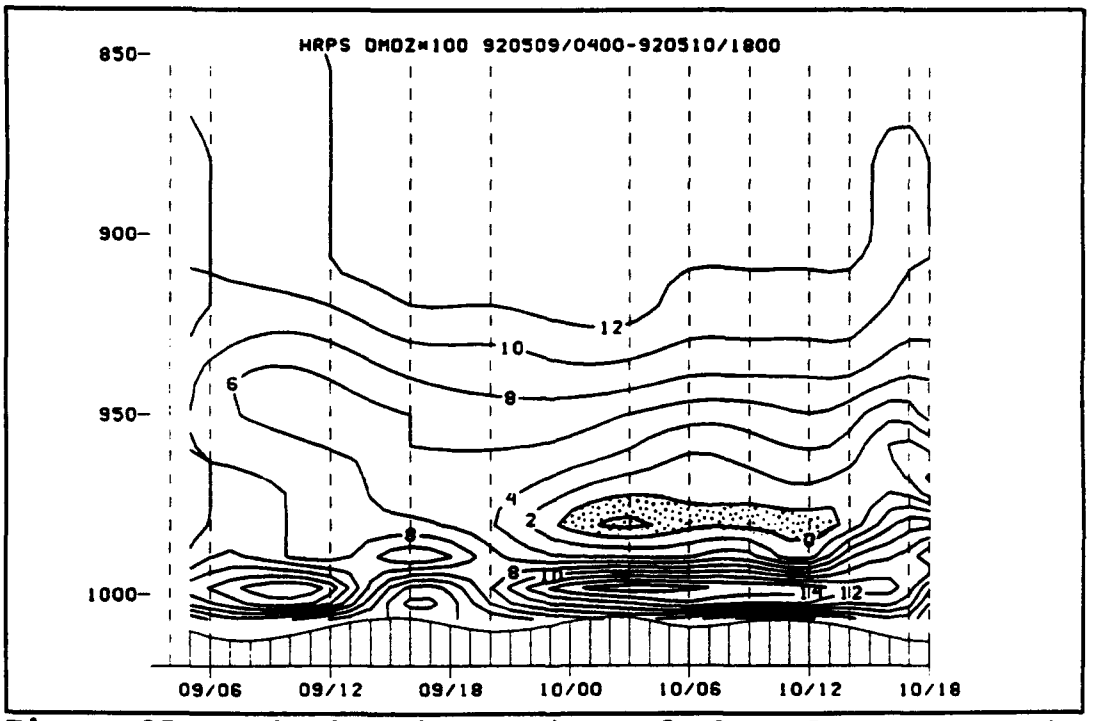

Figure 35: dM/dZ timesection of GB-HIS measurements from 9-10 May 1992 during the PTSUR 1992 cruise.

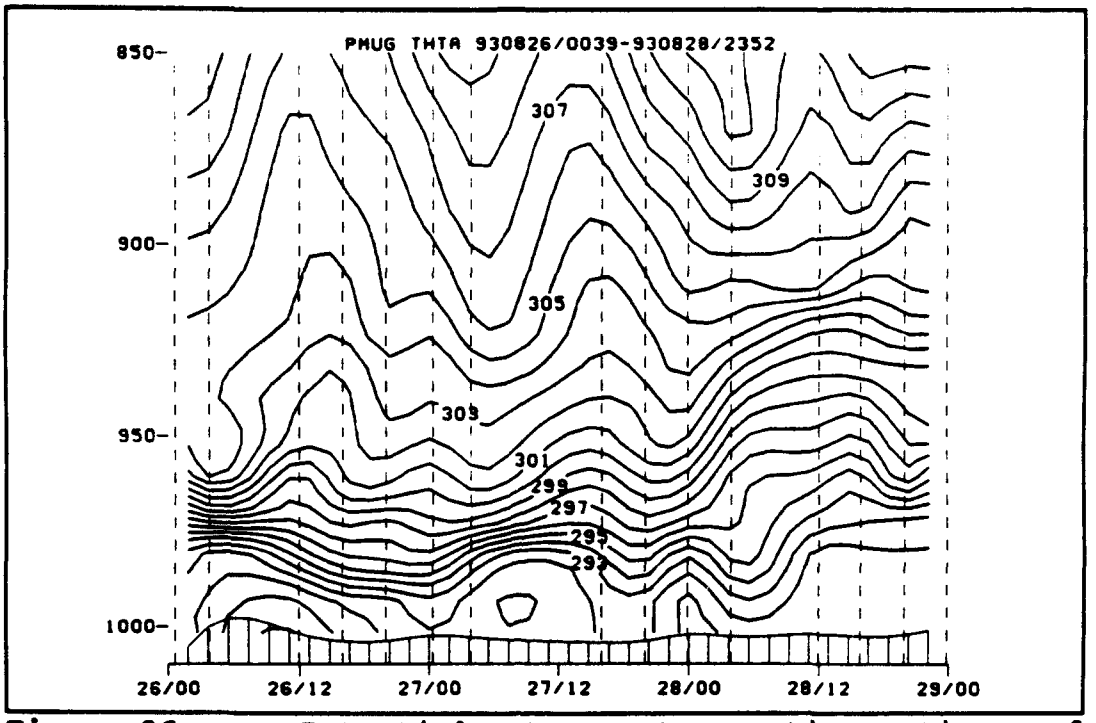

Figure 36: Potential temperature timesection of radiosonde observations from 26-28 August 1993 during VOCAR at PTMUGU.

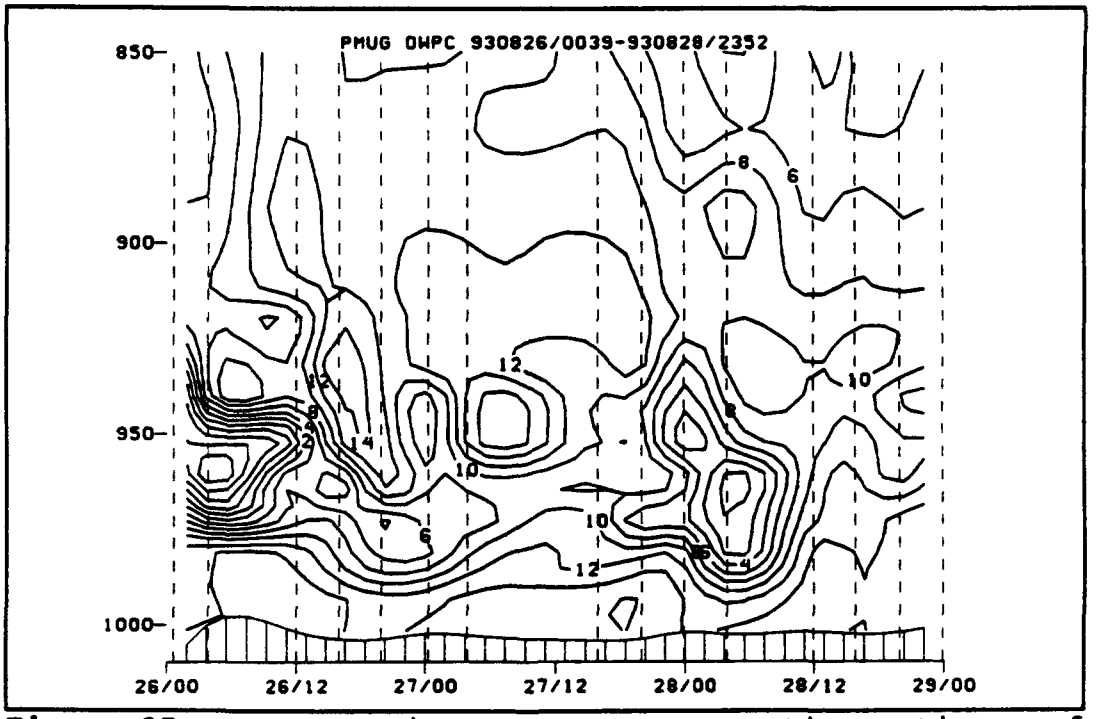

Figure 37: Dewpoint temperature timesection of radiosonde observations from 26-28 August 1993 during VOCAR at PTMUGU.

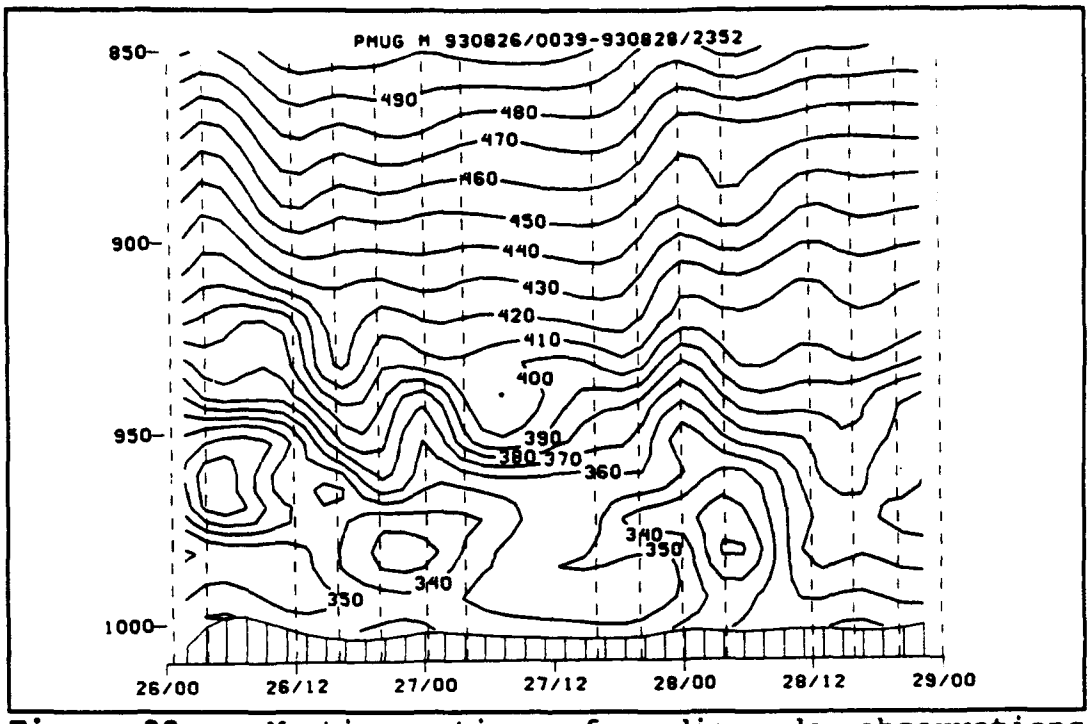

Figure 38: M timesection of radiosonde observations from 26-28 August 1993 during VOCAR at PTMUGU.

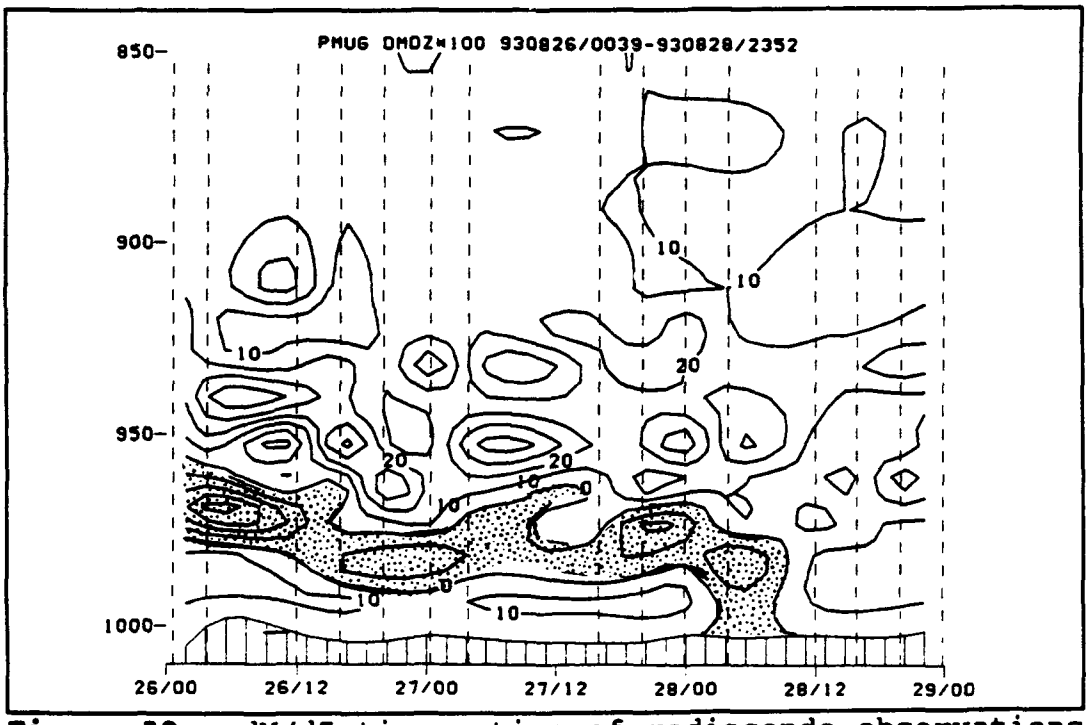

Figure 39: dM/dZ timesection of radiosonde observations from 26-28 August 1993 during VOCAR at PTMUGU.

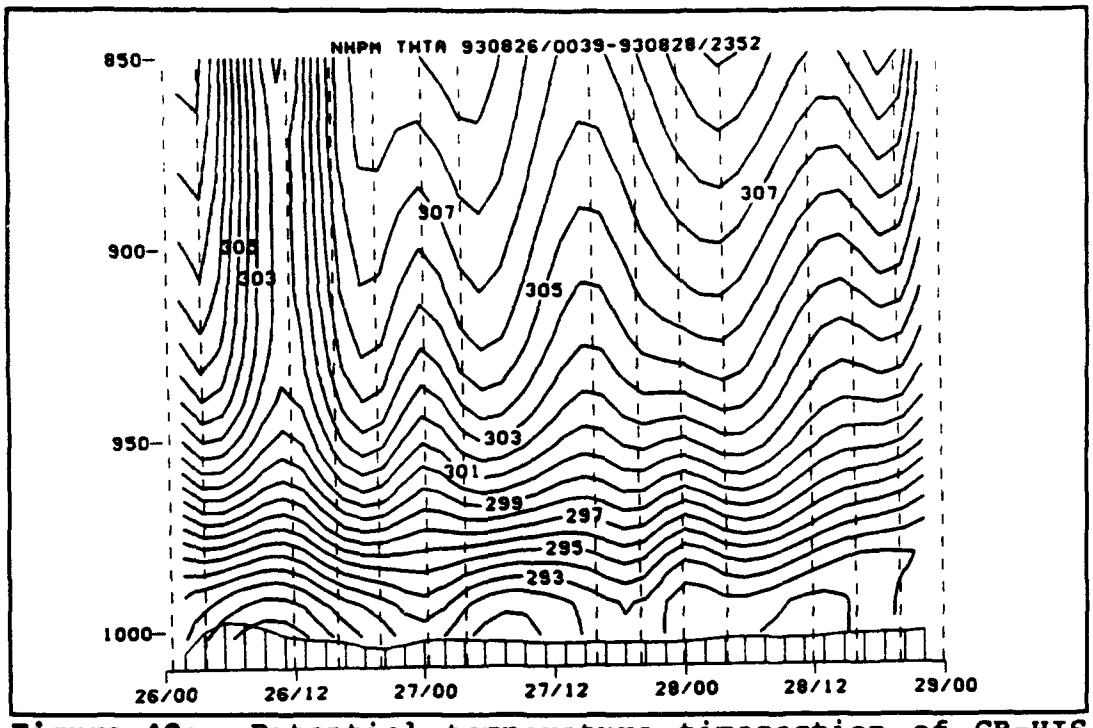

Figure 40: Potential temperature timesection of GB-HIS measurements from 26-28 August 1993 during VOCAR at PTMUGU.

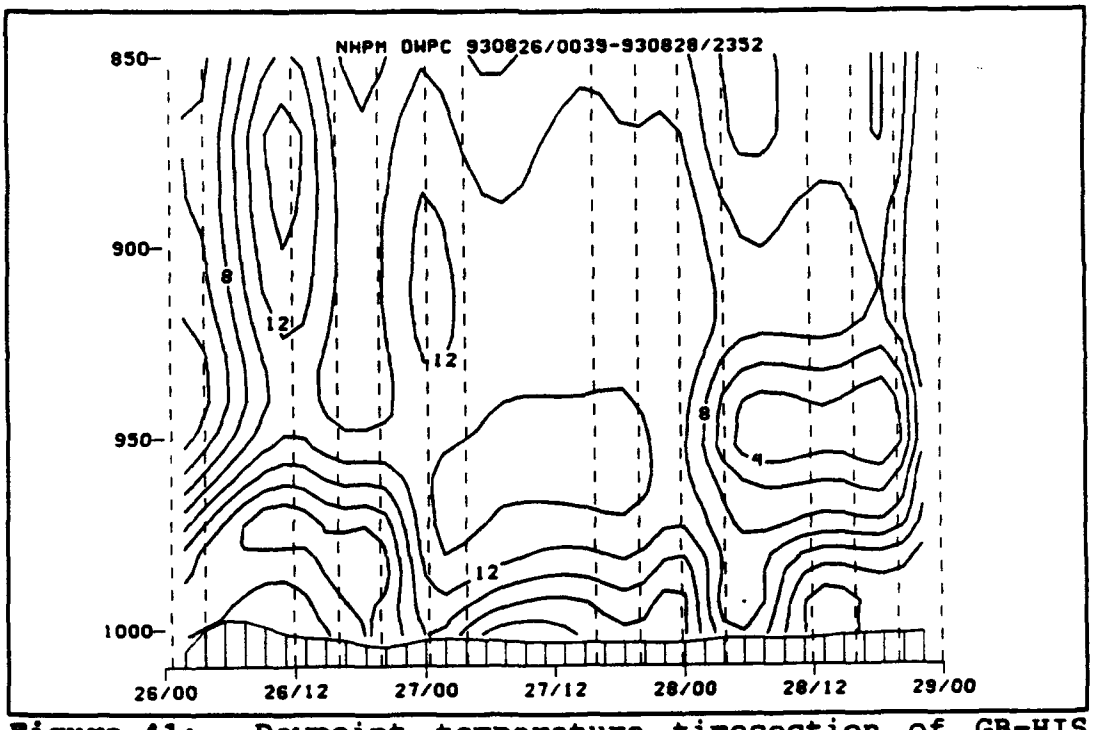

Figure 41: Dewpoint temperature timesection of GB-HIS measurements from 26-28 August 1993 during VOCAR at PTMUGU.

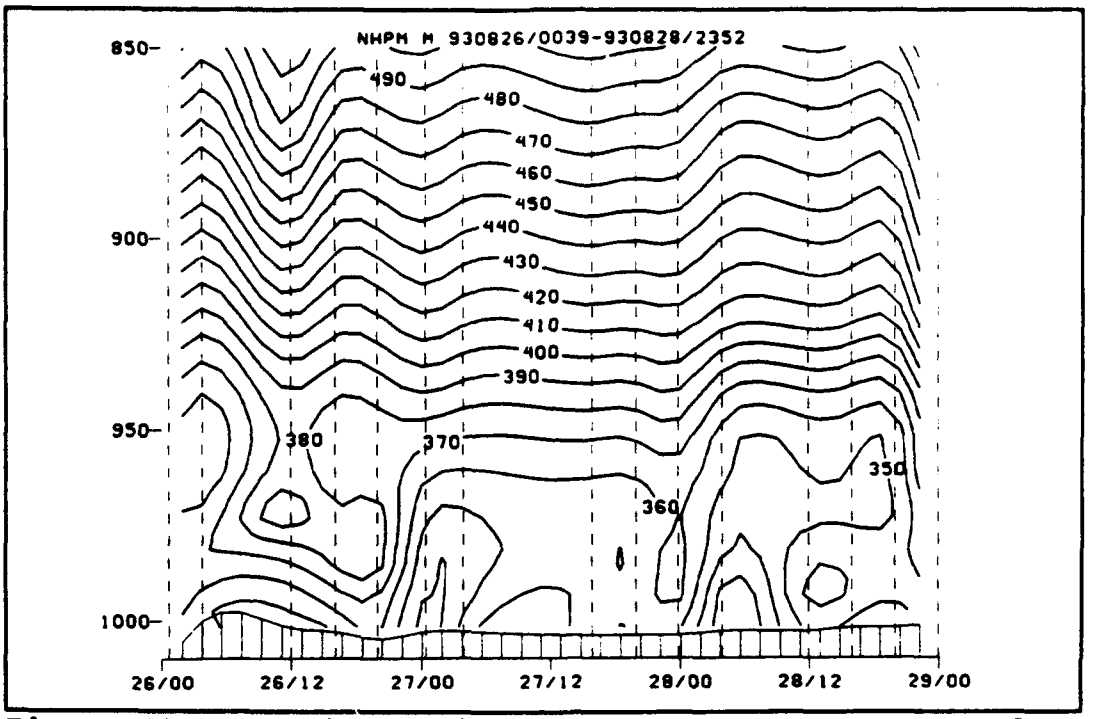

Figure 42: M timesection of GB-HIS measurements from 26-28 August 1993 during VOCAR at PTMUGU.

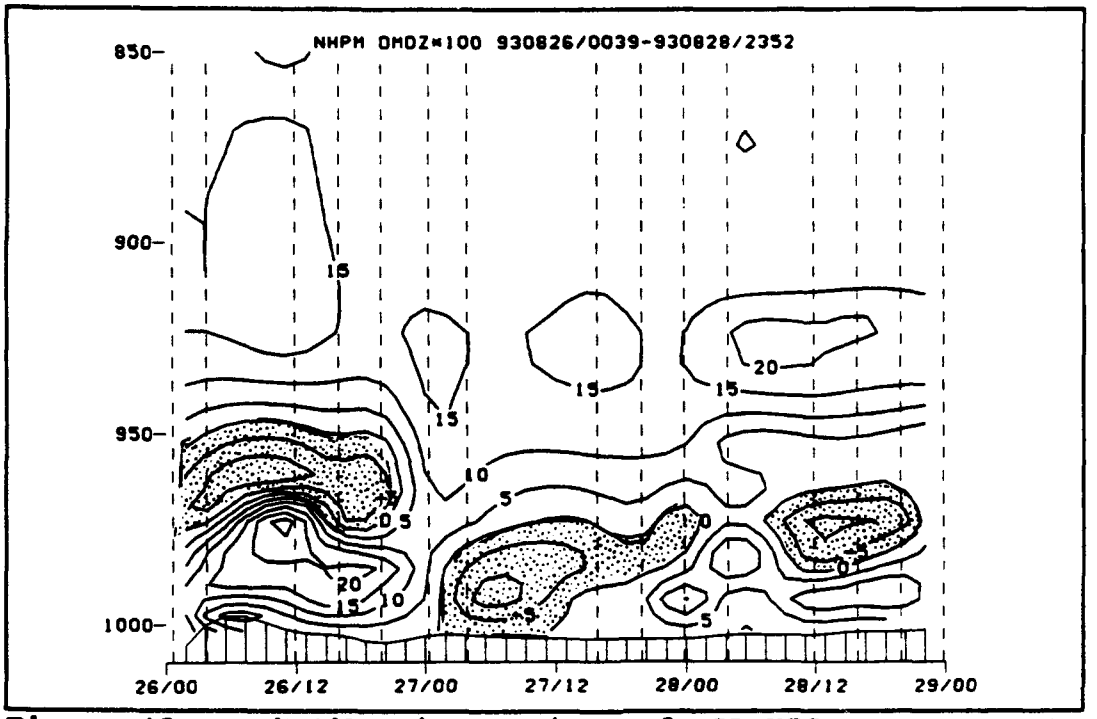

Figure 43: dM/dZ timesection of GB-HIS measurements from 26-28 August 1993 during VOCAR at PTMUGU.

LIST OF REFERENCES

Clough, S.A., Worsham, R.D., Smith, W.L., Revercomb, H.E., Knuteson, R.O., Woolf, H.W., Anderson, G.P., Hoke, M.L., and F.X. Kneizys, 1988: Validation of FASCODE calculations with HIS spectral radiance measurements. International Radiation Symposium, Lille, France, 18-24 August.

Ding, H., 1993: An evaluation of the utility of Ground-Based High Resolution Interferometer (GB-HIS) soundings of the planetary boundary layer. Master's thesis, University of Wisconsin-Madison, pp. 1-80.

Knuteson, R.G., 1993: University of Wisconsin participation in the VOCAR experiment at Pt Mugu, California: Preliminary results. University of Wisconsin-Madison, pp. 1-23.

Martinez, A.A., 1991: High frequency analyses of coastal meteorological phenomena affecting refractivity. Master's thesis, Naval Postgraduate School, Monterey, California, pp. 1-87.

Rao, P.K., Holmes, S.J., Anderson, R.K., Winston, J.S., and P.E. Lehr, 1990: Weather Satellites: Systems, Data, and Environmental Applications. American Meteorological Society, p. 109.

Revercomb, H.E., 1993: Background for IOTA investigation of HIS. University of Wisconsin-Madison, pp. 1-14.

Rugg, S.A., 1992: An investigation of the Ground-Based High-Resolution Interferometer Sounder (GB-HIS) in a coastal marine environment. Master's thesis, Naval Postgraduate School, Monterey, California, pp. 1-91.

Smith, W.L., Revercomb, H.E., Howell, H.B., Woolf, H.M., Knuteson, R.O., Decker, R.G., Lynch, E.R., Westwater, R.G., Strauch, K.P., Morgan, B., Stankov, M.J., Falls, J., Jordan, M., Jacobsen, W.F., Dabberdt, W.F., McBeth, R., Albright, G., Paneitz, C., Wright, G., May, P.T., and M.T. Decker, 1990: GAPEX: A ground-based atmospheric profiling experiment. Bulletin of American Meteorological Society, 71, pp. 310-318.

Smith, W.L., Revercomb, H.E., Howell, Huang, H.L., Knuteson, R.O., Koenig, E.W., LaPorte, D.D., Silverman,S., Sromovsky, L.A., and H.M. Woolf, 1990: GHIS - The GOES high-resolution interferometer sounder. Journal of Applied Meteorology, **29**, pp. 1189-1204.

Smith, W.L., Revercomb, H.E., Knuteson, R.O., Howell, H.B., and F.A. Best, 1993: Remote sensing of the planetary boundary layer with a high-resolution interferometer sounder. Submitted to Journal of Applied Meteorology.

INITIAL DISTRIBUTION LIST

		No. Copies
1.	Defense Technical Information Center Cameron Station Alexandria VA 22304-6145	2
2.	Library, Code 052 Naval Postgraduate School Monterey CA 93943-5002	2
3.	Chairman (Code MR/HY) Department of Meteorology Naval Postgraduate School Monterey, CA 93943-5114	1
4.	Chairman (Code OC/Co) Department of Oceanography Naval Postgraduate School Monterey, CA 93943-5122	1
5.	Professor Carlyle H. Wash (Code MR/WX) Department of Meteorology Naval Postgraduate School Monterey, CA 93943-5114	1
6.	Professor Kenneth L. Davidson (Code MR/WX) Department of Meteorology Naval Postgraduate School Monterey, CA 93943-5114	1
7.	Lieutenant Roy R. Ledesma PSC 819, Box 31 FPO AE 09645-3200	1
8.	Director Naval Oceanography Division Naval Observatory 34th and Massachusetts Avenue NW Washington, DC 20390	1
9.	Commander Naval Oceanography Command Stennis Space Center, MS 39529-5000	1

10. Professor William L. Smith
SSEC, University of Wisconsin
1225 W. Dayton Street
Madison, WI 53706 — 1

11. Professor Robert O. Knuteson
SSEC, University of Wisconsin
1225 W. Dayton Street
Madison, WI 53706 — 1

12. Mr. Wayne Feltz
SSEC, University of Wisconsin
1225 W. Dayton Street
Madison, WI 53706 — 1